

FLEXIBLE ENLARGED CONJUGATE GRADIENT METHODS

SOPHIE MOUFAWAD *

Abstract. Enlarged Krylov subspace methods and their s -step versions were introduced [7] in the aim of reducing communication when solving systems of linear equations $Ax = b$. These enlarged CG methods consist of enlarging the Krylov subspace by a maximum of t vectors per iteration based on the domain decomposition of the graph of A . As for the s -step versions, s iterations of the enlarged Conjugate Gradient methods are merged in one iteration. The Enlarged CG methods and their s -step versions converge in less iterations than the classical CG, but at the expense of requiring more memory storage than CG. Thus in this paper we explore different options for reducing the memory requirements of these enlarged CG methods without affecting much their convergence.

Key words. Linear Algebra, Iterative Methods, Krylov subspace methods, Conjugate Gradient methods, High Performance Computing, Minimizing Communication

1. Introduction. Conjugate Gradient (CG) [11] is a well-known Krylov subspace iterative method used for solving systems of linear equations $Ax = b$ with $n \times n$ symmetric positive definite (spd) sparse matrices A . Other Krylov subspace methods that solve general systems are Generalized Minimal Residual (GMRES) [22], bi-Conjugate Gradient [15, 6], and bi-Conjugate Gradient Stabilized [23]. CG is known for its short recurrence relations for defining the approximate solution $x_k \in x_0 + \mathcal{K}_k(A, r_0)$ at the k^{th} iteration, where $\mathcal{K}_k(A, r_0) = \{r_0, Ar_0, \dots, A^{k-1}r_0\}$ is the Krylov subspace of dimension at most k , $r_0 = b - Ax_0$ is the initial residual, and x_0 is the initial iterate or guess. This short recurrence leads to limited memory requirements (4 vectors of length n and sparse matrix A). However, CG iterations consist of BLAS 1 operations, specifically dot products and SAXPY's, and one BLAS2 operation, GAXPY or matrix-vector multiplication. Thus, when implementing CG on modern computer architectures, communication is a bottleneck in these BLAS operations due to technological reasons [14], where communication refers to data movement between different levels of memory hierarchy (sequential) and different processors/cores (parallel).

Different approaches have been adopted to reduce this effect such as pipelining communication and computation in order to hide communication [4, 9], or replacing BLAS1 and BLAS2 operations by denser operations that may be parallelized more efficiently with less communication. The latter can be achieved using different strategies. The first is to merge s iterations of CG to obtain the s -step method [24, 3]. Moreover, communication avoiding methods [12], which are based on s -step methods, introduce communication avoiding kernels that further reduce communication, even if at the expense of performing redundant computations. Other variants of s -step CG methods were introduced like [1]. The second strategy is to introduce new variants of CG by using different and larger Krylov subspaces, such as augmented CG [2, 21, 5], block CG [19], and enlarged CG [7, 17] that are based on augmented, block, and enlarged Krylov subspaces, respectively. For a detailed comparison between these methods, refer to [18].

Several Enlarged Krylov subspace Conjugate Gradient methods were introduced [7, 17] with the goal of obtaining methods that converge faster than classical Krylov methods in terms of iterations and consequently parallel runtime, by performing denser operations per iteration that require less communications when parallelized. These methods approximate the solution of the system $Ax = b$ iteratively by a sequence of vectors $x_k \in x_0 + \mathcal{K}_{k,t}(A, r_0)$ ($k > 0$), obtained by imposing the Petrov-Galerkin condition, $r_k \perp \mathcal{K}_{k,t}(A, r_0)$, where $\mathcal{K}_{k,t}(A, r_0)$ is the enlarged Krylov subspace of dimension at most tk . $\mathcal{K}_{k,t}(A, r_0)$ is based on a domain

*American University of Beirut (AUB), Beirut, Lebanon. (sm101@aub.edu.lb)

decomposition of A into t disjoint subdomains, δ_i with $\delta = \bigcup_{i=1}^t \delta_i = \{1, 2, \dots, n\}$, and for $i \neq j$, $\delta_i \cap \delta_j = \phi$

$$\begin{aligned} \mathcal{K}_{k,t}(A, r_0) &= \text{span}\{T^t(r_0), AT^t(r_0), A^2T^t(r_0), \dots, A^{k-1}T^t(r_0)\} \\ &= \text{span}\{T_1^t(r_0), T_2^t(r_0), \dots, T_t^t(r_0), \\ &\quad AT_1^t(r_0), AT_2^t(r_0), \dots, AT_t^t(r_0), \\ &\quad \dots, \\ &\quad A^{k-1}T_1^t(r_0), A^{k-1}T_2^t(r_0), \dots, A^{k-1}T_t^t(r_0)\}. \end{aligned}$$

$T^t(r_0) = \{T_1^t(r_0), T_2^t(r_0), \dots, T_t^t(r_0)\}$ is an operator that splits r_0 into t vectors, with $T_i^t(r_0)$ being the operator that projects vector r_0 on subdomain i of matrix A , δ_i . The matrix $[T^t(v)]$ is shown in (4.1).

The enlarged CG versions introduced in [7] are MSDO-CG, LRE-CG, SRE-CG, SRE-CG2, and the truncated SRE-CG2. Note that in [8] a block CG method based on SRE-CG is proposed, whereby one system with multiple right-hand sides is solved by defining R_0 using the enlarged Krylov subspace, i.e. $R_0 = [T^t(r_0)]$, and the solution of $Ax = b$ is the sum of the block solution X_k . The enlarged CG versions introduced in [7] perform block operations, yet they are not Block methods as they do not solve a system with multiple right-hand sides. Moreover, the residual vectors $r_k = b - Ax_k$ are not orthogonal to the enlarged Krylov subspace by definition. Hence the need for A-orthonormalizing the basis vectors to impose the Petrov-Galerkin condition.

Recently, s-step Enlarged CG versions were introduced [18] by merging s iterations of the enlarged CG methods. As shown in [7] and [18] the Enlarged CG methods and their s-step versions converge in less iterations than the classical CG, but at the expense of requiring more memory storage than CG. Thus in this paper we explore different options for reducing the memory requirements of these enlarged CG methods, specifically SRE-CG2 (section 2.1) and MSDO-CG (section 2.2), without affecting much their convergence. Apart from the truncated versions introduced in [7] and the well-known restarting versions (section 3), we introduce flexible enlarged versions (section 4) where after some iteration (to be determined) the number of computed basis vectors is reduced to half. Then, all these versions are tested in section 5, to check their convergence along with the reduced memory requirements.

2. Enlarged CG Methods. The enlarged CG methods are projection iterative methods that seek at iteration k an approximate solution to the $n \times n$ system of linear equations $Ax = b$ from the enlarged Krylov Subspace by imposing the Petrov-Galerkin constraint on the k^{th} residual r_k ,

1. Subspace Condition $x_k \in x_0 + \mathcal{K}_{k,t}(A, r_0)$
2. Orthogonality Condition $r_k \perp \mathcal{K}_{k,t}(A, r_0)$

where x_0 is the initial guess, $r_0 = b - Ax_0$ the initial residual, and $r_k = b - Ax_k$. The enlarged Krylov subspace is based on a domain decomposition of the matrix A , where the index domain $\delta = \{1, 2, \dots, n\}$ is divided into t disjoint subdomains δ_i , with $\delta_i \cap \delta_j = \phi$ for $i \neq j$, and $\delta = \bigcup_{i=1}^t \delta_i$. Then, the enlarged Krylov subspace is given by

$$\mathcal{K}_{k,t}(A, r_0) = \text{span}\{T^t(r_0), AT^t(r_0), \dots, A^{k-1}T^t(r_0)\},$$

where $T^t(r_0)$ is an operator that projects r_0 on the t subdomains δ_i producing a set of t vectors $\{T_1^t(r_0), T_2^t(r_0), \dots, T_t^t(r_0)\}$ as shown in (4.1) with $T_j^t(r_0)$ being the operator that projects r_0 on the subdomain δ_j .

2.1. SRE-CG2. The short recurrence enlarged CG versions are iterative enlarged Krylov subspace projection methods that build at the k^{th} iteration, an A-orthonormal candidate basis Q_k ($Q_k^T A Q_k = I$) for the enlarged Krylov subspace $\mathcal{K}_{k,t}(A, r_0)$ and approximate the solution, $x_k = x_{k-1} + Q_k \alpha_k$, by imposing the orthogonality condition on $r_k = r_{k-1} - A Q_k \alpha_k$, ($r_k \perp \mathcal{K}_{k,t}$). Then, $\alpha_k = (Q_k^T A Q_k)^{-1} (Q_k^T r_k)$ is obtained by minimizing $\phi(x_{k-1} + Q_k \alpha)$ where Q_k is an $n \times kt$ matrix, \cdot^T denotes the transpose of a matrix, and

$$\phi(x) = \frac{1}{2} x^T A x - x^T b.$$

It was proven in [7] that at each iteration $k \geq 4$, the t newly computed basis vectors $W_k = A W_{k-1}$ are A-orthogonal to W_i for $i \leq k-3$, where $W_1 = [T^t(r_0)]$ is the matrix containing the t vectors of $T^t(r_0)$. This leads to a short recurrence in $x_k = x_{k-1} + W_k \alpha_k$ and $r_k = r_{k-1} - A W_k \alpha_k$, where $\alpha_k = W_k^T r_{k-1}$. Moreover, W_k has to be A-orthonormalized only against W_{k-1} and W_{k-2} using CGS2 A-orthonormalization method (Algorithm 18, [17]), and then against itself using A-CholQR [20] or Pre-CholQR [16, 17]. This is the SRE-CG method that requires storing at most three block vectors W_{k-2}, W_{k-1}, W_k .

However, in finite arithmetic there is a loss of A-orthogonality at the k^{th} iteration between the vectors of $Q_k = [W_1, W_2, \dots, W_k]$ which is reflected on the number of iterations needed till convergence in the SRE-CG method. Moreover, once $W_k = A W_{k-1}$ is A-orthonormalized against all previous W_i 's for $i = 1, 2, \dots, k-1$ in the SRE-CG2 method (Algorithm 1), the number of iterations was vastly reduced as compared to SRE-CG. Yet, this comes at the expense of performing more operations for the A-orthonormalization per iteration and requiring more memory storage, specifically storing all the block vectors W_1, W_2, \dots, W_k .

Algorithm 1 SRE-CG2

Input: A , $n \times n$ symmetric positive definite matrix; k_{max} , maximum allowed iterations
 b , $n \times 1$ right-hand side; x_0 , initial guess; ϵ , stopping tolerance

Output: x_k , approximate solution of the system $Ax = b$

- 1: $r_0 = b - Ax_0$, $\rho_0 = \|r_0\|_2$, $k = 1$;
 - 2: **while** ($\rho_{k-1} > \epsilon \rho_0$ and $k < k_{max}$) **do**
 - 3: **if** ($k == 1$) **then**
 - 4: A-orthonormalize $W_k = [T^t(r_{k-1})]$, and let $Q = W_k$
 - 5: **else**
 - 6: Let $W_k = A W_{k-1}$
 - 7: A-orthonormalize W_k against Q
 - 8: A-orthonormalize W_k and let $Q = [Q \ W_k]$
 - 9: **end if**
 - 10: $\alpha_k = W_k^T r_{k-1}$
 - 11: $x_k = x_{k-1} + W_k \alpha_k$
 - 12: $r_k = r_{k-1} - A W_k \alpha_k$
 - 13: $\rho_k = \|r_k\|_2$, $k = k + 1$
 - 14: **end while**
-

2.2. MSDO-CG. The MSDO-CG method [7] computes search directions that belong to the enlarged Krylov Subspace $\mathcal{K}_{k,t}(A, r_0)$, rather than computing basis vectors. Specifically, at each iteration k , t search directions P_k are computed as in (2.1) and then A-orthonormalized against all P_i 's ($i < k$), to impose the orthogonality condition on $r_k = r_{k-1} - A P_k \alpha_k$.

$$\begin{cases} P_k = \mathcal{T}_{k-1}^t + P_{k-1} \text{diag}(\beta_k) \\ P_0 = \mathcal{T}_0^t \end{cases} \quad (2.1)$$

where $\beta_k = -P_{k-1}^T A r_{k-1}$, and $\mathcal{T}_i^t = [T^t(r_i)]$ is the matrix containing the t vectors of $T^t(r_i)$. Then, the approximate solution is defined as $x_k = x_{k-1} + P_k \alpha_k$, where $\alpha_k = P_k^T r_{k-1}$ is computed by minimizing $\phi(x_{k-1} + P_k \alpha)$, as shown in Algorithm 2.

Algorithm 2 MSDO-CG

Input: A , $n \times n$ symmetric positive definite matrix; k_{max} , maximum allowed iterations
 b , $n \times 1$ right-hand side; x_0 , initial guess; ϵ , stopping tolerance
Output: x_k , approximate solution of the system $Ax = b$

```

1:  $r_0 = b - Ax_0$ ,  $\rho_0 = \|r_0\|_2$ ,  $k = 1$ ,
2: while ( $\rho_{k-1} > \epsilon \rho_0$  and  $k < k_{max}$ ) do
3:   if ( $k == 1$ ) then
4:     A-orthonormalize  $P_1 = [T^t(r_{k-1})]$ , let  $V_1 = AP_1$  and  $Q = P_1$ 
5:   else
6:     Let  $\beta_k = -V_{k-1}^T r_{k-1}$ 
7:     Let  $P_k = [T^t(r_{k-1})] + P_{k-1} \text{diag}(\beta_k)$ 
8:     A-orthonormalize  $P_k$  against  $Q$ 
9:     A-orthonormalize  $P_k$ , let  $V_k = AP_k$  and  $Q = [Q \ P_k]$ 
10:  end if
11:   $\alpha_k = P_k^T r_{k-1}$ 
12:   $x_k = x_{k-1} + P_k \alpha_k$ 
13:   $r_k = r_{k-1} - V_k \alpha$ 
14:   $\rho_k = \|r_k\|_2$ ,  $k = k + 1$ 
15: end while

```

In [18], with the aim of introducing s-step versions of the enlarged CG method, a modified MSDO-CG was introduced that searches for the solution in the modified Krylov subspace

$$\begin{aligned} x_k &\in x_0 + \overline{\mathcal{K}}_{k,t}(A, r_0) \\ \overline{\mathcal{K}}_{k,t}(A, r_0) &= \text{span} \{T^t(r_0), T^t(r_1), \dots, T^t(r_{k-1})\} \end{aligned}$$

by building an A-orthonormal basis similarly to SRE-CG2, with the difference that at each iteration $W_k = [T^t(r_{k-1})]$. Thus, the Modified MSDO-CG algorithm is the same as the SRE-CG2 algorithm 1 with the exception of line 6 that is replaced by:

$$\text{Let } W_k = [T^t(r_{k-1})].$$

At iteration k in both MSDO-CG and modified MSDO-CG algorithms, there is a need to A-orthonormalize a block of t vectors, be it P_k or W_k , against all $k - 1$ previous blocks of t vectors. Thus, there is a need to store all these k block vectors, even though we have short recurrence formulae for x_k and r_k .

3. Truncated and Restarted Enlarged CG methods. In the three methods, SRE-CG2, MSDO-CG, and Modified MSDO-CG, the iterates have short recurrence formulae. However, due to the A-orthonormalization process there is a need to store all the generated block vectors. One option is to truncate the A-orthonormalization process by A-orthonormalizing W_k against the previous *trunc* blocks only, for $2 \leq \text{trunc} \leq k_{max}$. Thus, requiring the storage of only the last *trunc* + 1 block vectors.

The truncated SRE-CG2 method was introduced in [7] to reduce the memory requirements of SRE-CG2. Note that for $trunc = 2$, we get the SRE-CG method, and for $trunc = k_{max}$ we get the SRE-CG2 method. The truncated SRE-CG2 algorithm differs from Algorithm 1 in line 8, where for $k > trunc$

$$Q = [W_{k-trunc+1}, W_{k-trunc+2}, \dots, W_k].$$

As for MSDO-CG or Modified MSDO-CG, it is possible to truncate the A-orthonormalization process similarly to SRE-CG2. The truncated MSDO-CG algorithm differs from Algorithm 2 in line 9, where for $k > trunc$

$$Q = [P_{k-trunc+1}, P_{k-trunc+2}, \dots, P_k].$$

Yet, unlike SRE-CG2, there is no guarantee that the method will converge, as theoretically there is a need for all the search directions P_k or all the basis vectors W_k to be A-orthonormal.

On the other hand, restarting SRE-CG2 or MSDO-CG or Modified MSDO-CG after j iterations implies that all the information obtained in the matrix Q is lost, be it the basis vectors of $\mathcal{K}_{j,t}$, or the search directions from $\mathcal{K}_{j,t}$ or the basis vectors of $\bar{\mathcal{K}}_{j,t}$ respectively. Then the last approximate solution x_j is used as an initial guess for the new cycle of j iterations. Thus, at most $j + 1$ block vectors are stored. However, for the stopping criteria we always compare to the initial residual ($\|r_k\|_2 / \|r_0\|_2 < tol$ for $k \geq j$). Thus, restarted SRE-CG2 algorithm and restarted MSDO-CG are respectively Algorithms 1 and 2 where line 3 is replaced by

if ($k \bmod j == 1$) then

Both truncated and restarted versions have the same fixed memory requirement for $j = trunc$. However, restarted versions requires less flops than their corresponding truncated versions, specifically in the A-orthonormalization (line 7 of Algorithm1, line 8 of Algorithm2), since after $j = trunc$ iterations the size of the Q matrix in the restarted versions varies from $n \times t$ to $n \times tj$, whereas it is fixed to $n \times tj$ in the truncated version.

Note that it is possible to restart SRE-CG2 and MSDO-CG not every j iterations, but once some measure of change in the residuals is less than a $restartTol$. We use, similarly to the flexible enlarged CG versions, the relative difference of the residual norm, i.e we restart once

$$\frac{|\|r_{k+1}\|_2 - \|r_k\|_2|}{\|r_0\|_2} < restartTol.$$

These restarted SRE-CG2 and restarted MSDO-CG are respectively Algorithms 1 and 2 where line 3 is replaced by

if ($k == 1$) or ($|\|r_{k+1}\|_2 - \|r_k\|_2| / \|r_0\|_2 < restartTol$) then

However, in this case the maximum needed memory requirement is not known beforehand, as the restarts will depend on the used $restartTol$ and the matrix at hand.

4. Flexible Enlarged CG methods. The concept behind “flexible” enlarged CG versions is that after some iterations k_F (to be determined) the number of computed vectors, be it basis vectors or search direction vectors, is reduced to half. This implies that at iteration $k_F + 1$ the $t/2$ computed basis or search direction vectors are based on the last residual r_{k_F} , specifically $T^{t/2}(r_{k_F})$. Similarly to $T^t(r_0)$, $T^{t/2}(r_{k_F})$ is the operator that projects the vector r_{k_F} over the $t/2$ subdomains δ_i where for $i = 1, 2, \dots, t/2$

$$\tilde{\delta}_i = \delta_{2i-1} \cup \delta_{2i} \quad \text{with} \quad \delta = \bigcup_{i=1}^{t/2} \tilde{\delta}_i = \bigcup_{i=1}^t \delta_i.$$

The comparison between the $n \times t$ matrix $[T^t(v)]$ and the $n \times t/2$ matrix $[T^{t/2}(v)]$ for some vector v that is partitioned into t parts is shown in (4.1)

$$v = \begin{bmatrix} * \\ \vdots \\ * \\ * \\ \vdots \\ * \\ \vdots \\ * \\ * \\ \vdots \\ * \\ * \\ \vdots \\ * \\ * \\ \vdots \\ * \\ * \end{bmatrix} \quad [T^t(v)] = \begin{bmatrix} * & 0 & 0 & 0 \\ \vdots & \vdots & \vdots & \vdots \\ * & 0 & 0 & 0 \\ 0 & * & \vdots & \vdots \\ \vdots & \vdots & \vdots & \vdots \\ 0 & * & 0 & 0 \\ \ddots & \ddots & \ddots & \ddots \\ 0 & 0 & * & 0 \\ \vdots & \vdots & \vdots & \vdots \\ 0 & 0 & * & 0 \\ 0 & 0 & 0 & * \\ \vdots & \vdots & \vdots & \vdots \\ 0 & 0 & 0 & * \end{bmatrix}_{n \times t} \quad [T^{t/2}(v)] = \begin{bmatrix} * & 0 \\ \vdots & \vdots \\ * & 0 \\ * & 0 \\ \vdots & \vdots \\ * & 0 \\ \vdots & \vdots \\ 0 & * \\ \vdots & \vdots \\ 0 & * \\ 0 & * \\ \vdots & \vdots \\ 0 & * \end{bmatrix}_{n \times \frac{t}{2}} \quad (4.1)$$

We start by defining the Flexible enlarged Krylov subspace and proving it is a superset to the Krylov subspace, then we define the switching condition and the flexible SRE-CG2 and MSDO-CG algorithms. Finally, we derive the preconditioned flexible SRE-CG2 and MSDO-CG methods.

4.1. Flexible Enlarged Krylov Subspace. With this reduction in dimension, the approximate solution x_k no longer belongs to the enlarged subspace $x_0 + \mathcal{K}_{k,t}(A, r_0)$, but it belongs to the flexible enlarged subspace

$$x_k \in \begin{cases} x_0 + \mathcal{K}_{k,t}(A, r_0), & \text{if } k \leq k_F \\ x_0 + \mathcal{K}_{k_F,t}(A, r_0) + \mathcal{K}_{k-k_F,t/2}(A, r_{k_F}), & \text{if } k > k_F \end{cases} \quad (4.2)$$

If the flexible enlarged method converges before k_F , then it is equivalent to the original enlarged method where $x_k \in x_0 + \mathcal{K}_{k,t}(A, r_0)$. In this case, as shown in [7] the Krylov subspace $\mathcal{K}_k(A, r_0) \subseteq \mathcal{K}_{k,t}(A, r_0)$, which validates the use of the enlarged Krylov subspace. If the flexible enlarged method converges in $k > k_F$ iterations, then we need to prove that the flexible enlarged Krylov Subspace is a superset to $\mathcal{K}_k(A, r_0)$. The following theorems lead to this conclusion.

THEOREM 4.1. *Let $1 \leq k_F < k$. Then, the Krylov subspace*

$$\mathcal{K}_k(A, r_0) = \mathcal{K}_{k_F}(A, r_0) + \mathcal{K}_{k-k_F}(A, r_{k_F})$$

where $r_{k_F} \in \mathcal{K}_{k_F+1}(A, r_0)$.

Proof. We prove that each set is subset of the other.

1. $\mathcal{K}_{k_F}(A, r_0) + \mathcal{K}_{k-k_F}(A, r_{k_F}) \subseteq \mathcal{K}_k(A, r_0)$:

Let $y \in \mathcal{K}_{k_F}(A, r_0) + \mathcal{K}_{k-k_F}(A, r_{k_F})$, then since $r_{k_F} = \sum_{j=1}^{k_F+1} c_j A^{j-1} r_0$

$$\begin{aligned} y &= \sum_{i=1}^{k_F} a_i A^{i-1} r_0 + \sum_{i=1}^{k-k_F} b_i A^{i-1} r_{k_F} = \sum_{i=1}^{k_F} a_i A^{i-1} r_0 + \sum_{i=1}^{k-k_F} \sum_{j=1}^{k_F+1} b_i c_j A^{i+j-2} r_0 \\ &= \sum_{i=1}^{k_F} a_i A^{i-1} r_0 + \sum_{i=1}^k \alpha_i A^{i-1} r_0 = \sum_{i=1}^k \tilde{\alpha}_i A^{i-1} r_0 \in \mathcal{K}_k(A, r_0) \end{aligned}$$

2. $\mathcal{K}_k(A, r_0) \subseteq \mathcal{K}_{k_F}(A, r_0) + \mathcal{K}_{k-k_F}(A, r_{k_F})$ by induction:

- Base Case: $k = k_F + 1$

Let $y \in \mathcal{K}_k(A, r_0)$, then

$$\begin{aligned} y &= \sum_{i=1}^{k_F+1} a_i A^{i-1} r_0 = \sum_{i=1}^{k_F} a_i A^{i-1} r_0 + a_k A^{k_F} r_0 \\ &= \sum_{i=1}^{k_F} a_i A^{i-1} r_0 + \frac{a_k}{c_k} r_{k_F} - \frac{a_k}{c_k} \sum_{j=1}^{k_F} c_j A^{j-1} r_0 \in \mathcal{K}_{k_F}(A, r_0) + \mathcal{K}_1(A, r_{k_F}) \end{aligned}$$

- Suppose that $\mathcal{K}_k(A, r_0) \subseteq \mathcal{K}_{k_F}(A, r_0) + \mathcal{K}_{k-k_F}(A, r_{k_F})$.
- Prove that $\mathcal{K}_{k+1}(A, r_0) \subseteq \mathcal{K}_{k_F}(A, r_0) + \mathcal{K}_{k-k_F+1}(A, r_{k_F})$.

Let $y_{k+1} \in \mathcal{K}_{k+1}(A, r_0)$, and $y_k \in \mathcal{K}_k(A, r_0) \subseteq \mathcal{K}_{k_F}(A, r_0) + \mathcal{K}_{k-k_F}(A, r_{k_F})$, then

$$\begin{aligned} y_{k+1} &= \sum_{i=1}^{k+1} a_i A^{i-1} r_0 = \sum_{i=1}^k a_i A^{i-1} r_0 + a_{k+1} A^k r_0 = \sum_{i=1}^k a_i A^{i-1} r_0 + a_{k+1} A^{k-k_F} A^{k_F} r_0 \\ &= \sum_{i=1}^k a_i A^{i-1} r_0 + \frac{a_{k+1}}{c_{k_F+1}} A^{k-k_F} r_{k_F} - \frac{a_{k+1}}{c_{k_F+1}} \sum_{j=1}^{k_F} c_j A^{k-k_F} A^{j-1} r_0 \\ &= \sum_{i=1}^k a_i A^{i-1} r_0 + \sum_{j=k-k_F+1}^k \tilde{c}_j A^{j-1} r_0 + \frac{a_{k+1}}{c_{k_F+1}} A^{k-k_F} r_{k_F} \\ &= \sum_{i=1}^{k_F} a_i A^{i-1} r_0 + \sum_{i=1}^{k-k_F} b_i A^{i-1} r_{k_F} + \frac{a_{k+1}}{c_{k_F+1}} A^{k-k_F} r_{k_F} = y_k + \frac{a_{k+1}}{c_{k_F+1}} A^{k-k_F} r_{k_F} \\ \implies y_{k+1} &= \sum_{i=1}^{k_F} a_i A^{i-1} r_0 + \sum_{i=1}^{k-k_F+1} b_i A^{i-1} r_{k_F} \in \mathcal{K}_{k_F}(A, r_0) + \mathcal{K}_{k-k_F+1}(A, r_{k_F}). \quad \square \end{aligned}$$

THEOREM 4.2. *The Krylov subspace $\mathcal{K}_k(A, v)$ is a subset of the enlarged Krylov subspace $\mathcal{X}_{k,t}(A, v)$ for any vector v and integer $t \geq 1$.*

Proof. Let $y \in \mathcal{K}_k(A, v)$, where $\mathcal{K}_k(A, v) = \{v, Av, \dots, A^{k-1}v\}$. Then,

$$y = \sum_{i=1}^k a_i A^{i-1} v = \sum_{i=1}^k a_i A^{i-1} [T^t(v)] * \mathbb{1}_t = \sum_{i=1}^k \sum_{j=1}^t a_i A^{i-1} T_j^t(v) \in \mathcal{X}_{k,t}(A, v)$$

since by definition (4.1) $v = [T^t(v)] * \mathbb{1}_t = [T_1^t(v) T_2^t(v) \cdots T_t^t(v)] * \mathbb{1}_t = \sum_{j=1}^t T_j^t(v)$. \square

As a corollary of theorems 4.1 and 4.2 we get the following result.

COROLLARY 4.3. *The Krylov subspace $\mathcal{K}_k(A, r_0)$ is a subset of the flexible enlarged Krylov subspace for $k > k_F$ and the even integer $t \geq 2$, i.e.*

$$\mathcal{K}_k(A, r_0) \subseteq \mathcal{X}_{k_F,t}(A, r_0) + \mathcal{X}_{k-k_F,t/2}(A, r_{k_F})$$

where $r_{k_F} \in \mathcal{K}_{k_F+1}(A, r_0)$.

Proof. By theorem 4.1, $\mathcal{K}_k(A, r_0) = \mathcal{K}_{k_F}(A, r_0) + \mathcal{K}_{k-k_F}(A, r_{k_F})$.

Moreover, by theorem 4.2, $\mathcal{K}_{k_F}(A, r_0) \subseteq \mathcal{X}_{k_F,t}(A, r_0)$ and $\mathcal{K}_{k-k_F}(A, r_{k_F}) \subseteq \mathcal{X}_{k-k_F,t/2}(A, r_{k_F})$, which completes the proof. \square

4.2. Switch. It remains to decide when to switch to computing half the basis vectors. One option is to fix k_F . However, given that it is not known before hand the number of iterations till convergence, a premature or late switch may have a negative effect on the convergence or end up with an unattained memory reduction. Thus, we suggest to switch once the relative difference of the residual norm is smaller than some predetermined switch tolerance

(switchTol), i.e. $\frac{\|r_{k+1}\|_2 - \|r_k\|_2}{\|r_0\|_2} < \text{switchTol}$.

This is based on the observation that the norm of the residual in the ECG methods may stagnate at several stages as shown in figures 4.1 for $t = 32$ partitions.

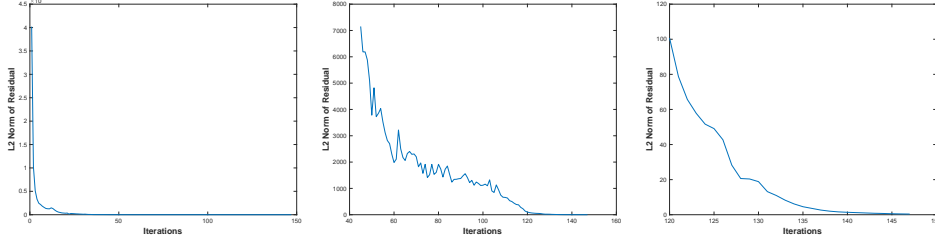


Fig. 4.1: Norm of residual vector for Ani3D matrix using SRE-CG2 for 32 partitions over all the 156 iterations needed to convergence, zoomed view from iteration 45, and zoomed view from iteration 120.

4.3. Flexible SRE-CG2 Algorithm. Applying this general flexible enlarged CG method to SRE-CG2 leads to Algorithm 3. The main difference with Algorithm 1 is that there is at most one iteration k where after which the dimension of W_j for $j \geq k$ is half that of W_{k-1} . This iteration $k = k_F + 1$ is when the relative difference of the residual norm is less than the given switchTol, and thus W_k is set to $[T^{1/2}(r_{k-1})]$. Specifically, line 6 in Algorithm 1 is replaced by lines 6-11 in Algorithm 3. This is similar to restarting with an initial guess set to x_{k-1} . Yet, the difference with restarted SRE-CG2 is that in the flexible version at the switch iteration W_k is A-orthonormalized against all the previous vectors.

Algorithm 3 Flexible SRE-CG2

Input: A , $n \times n$ symmetric positive definite matrix; k_{max} , maximum allowed iterations
 b , $n \times 1$ right-hand side; x_0 , initial guess; ϵ , stopping tolerance; switchTol

Output: x_k , approximate solution of the system $Ax = b$

- 1: $r_0 = b - Ax_0$; $\rho_0 = \|r_0\|_2$; $counter = 0$; $tol1 = 1$; $k = 1$;
 - 2: **while** ($\rho_{k-1} > \epsilon \rho_0$ and $k < k_{max}$) **do**
 - 3: **if** ($k == 1$) **then**
 - 4: A-orthonormalize $W_k = [T^t(r_0)]$, and let $Q = W_k$
 - 5: **else**
 - 6: **if** ($tol1 < switchTol$ and $counter == 0$) **then**
 - 7: $W_k = [T^{t/2}(r_{k-1})]$;
 - 8: $counter = 1$;
 - 9: **else**
 - 10: Let $W_k = AW_{k-1}$;
 - 11: **end if**
 - 12: A-orthonormalize the vectors of W_k against Q ;
 - 13: A-orthonormalize the vectors of W_k and let $Q = [Q, W_k]$;
 - 14: **end if**
 - 15: $\alpha_k = W_k^T r_{k-1}$;
 - 16: $x_k = x_{k-1} + W_k \alpha_k$;
 - 17: $r_k = r_{k-1} - AW_k \alpha_k$;
 - 18: $\rho_k = \|r_k\|_2$; $tol1 = (\rho_k - \rho_{k-1})/\rho_0$; $k = k + 1$;
 - 19: **end while**
-

4.4. Flexible MSDO-CG Algorithm. Applying the idea of flexible enlarged CG methods to the case of MSDO-CG leads to algorithm 4. Once the relative difference of the residual norm is less than the given switchTol, the number of introduced search directions at iteration k is halved by setting $P_k = [T^{t/2}(r_{k-1})]$ and A-orthonormalizing it against all previous search directions. Thus, lines 6-7 in algorithm 2 are replaced by lines 6-14 in algorithm 4.

Algorithm 4 Flexible MSDO-CG

Input: A , $n \times n$ symmetric positive definite matrix; k_{max} , maximum allowed iterations
 b , $n \times 1$ right-hand side; x_0 , initial guess; ϵ , stopping tolerance; switchTol

Output: x_k , approximate solution of the system $Ax = b$

```

1:  $r_0 = b - Ax_0$ ,  $\rho_0 = \|r_0\|_2$ ,  $counter = 0$ ;  $tol1 = 1$ ;  $k = 1$ ;
2: while ( $\rho_{k-1} > \epsilon \rho_0$  and  $k < k_{max}$ ) do
3:   if ( $k == 1$ ) then
4:     A-orthonormalize  $P_1 = [T^t(r_0)]$ , let  $V_1 = AP_1$  and  $Q = P_1$ 
5:   else
6:     if ( $tol1 < switchTol$  and  $counter == 0$ ) then
7:        $P_k = [T^{t/2}(r_{k-1})]$ ;
8:        $counter = 1$ ;
9:     else
10:      Let  $\beta_k = -V_{k-1}^T r_{k-1}$ 
11:      if ( $counter == 0$ ) then Let  $P_k = [T^t(r_{k-1})] + P_{k-1}diag(\beta_k)$ 
12:      else Let  $P_k = [T^{t/2}(r_{k-1})] + P_{k-1}diag(\beta_k)$ 
13:      end if
14:    end if
15:    A-orthonormalize  $P_k$  against  $Q$ 
16:    A-orthonormalize  $P_k$ , let  $V_k = AP_k$  and  $Q = [Q P_k]$ 
17:    end if
18:     $\alpha_k = P_k^T r_{k-1}$ 
19:     $x_k = x_{k-1} + P_k \alpha_k$ 
20:     $r_k = r_{k-1} - V_k \alpha_k$ 
21:     $\rho_k = \|r_k\|_2$ ,  $tol1 = (\rho_k - \rho_{k-1})/\rho_0$ ;  $k = k + 1$ 
22: end while

```

4.5. Preconditioned versions. Conjugate Gradient solves systems $Ax = b$ with symmetric positive definite (spd) matrices A . Thus, preconditioned matrix \hat{A} should also be spd. Hence split preconditioning is used, where the preconditioner $M = LL^T$ and the preconditioned matrix $\hat{A} = L^{-1}AL^{-T}$ are spd. Then, the equivalent preconditioned system is

$$\hat{A}\hat{x} = \hat{b} \quad (4.3)$$

where $\hat{x} = L^T x$ and $\hat{b} = L^{-1}b$.

The first option discussed in [17], is to first solve $\hat{A}\hat{x} = \hat{b}$ by replacing A by $\hat{A} = L^{-1}AL^{-T}$ and b by $\hat{b} = L^{-1}b$ in the algorithms. Then, the solution x is obtained by solving $\hat{x} = L^T x$. The first implication is that the A-orthonormalization is replaced by $L^{-1}AL^{-T}$ -orthonormalization (Algorithms 19 and 22 of [17]). The second is the need to replace every matrix-vector multiplication Ax by $y_3 = \hat{A}\hat{x} = L^{-1}AL^{-T}\hat{x}$ which requires solving $L^T y_1 = \hat{x}$, computing $y_2 = Ay_1$ and solving $Ly_3 = y_2$. Assuming L is lower triangular, then this requires a sequence of backward substitution, matrix-vector multiplication and forward substitution.

The second option discussed in [18] is to avoid using the $L^{-1}AL^{-\top}$ -orthonormalization and modifying the recurrence relations of α_k, x_k, r_k in preconditioned algorithms 3 and 4.

Given system (4.3), then the corresponding recurrence relations for both preconditioned flexible SRE-CG2 and MSDO-CG are:

$$\begin{aligned}\hat{\alpha}_k &= \hat{Z}_k^\top \hat{r}_{k-1} \\ \hat{x}_k &= \hat{x}_{k-1} + \hat{Z}_k \hat{\alpha}_k \\ \hat{r}_k &= \hat{r}_{k-1} - \hat{A} \hat{Z}_k \hat{\alpha}_k\end{aligned}$$

where \hat{Z}_k is \hat{A} -orthonormalized against \hat{Z}_i , i.e. $\hat{Z}_k^\top \hat{A} \hat{Z}_i = 0$ and $\hat{Z}_i^\top \hat{A} \hat{Z}_i = I$. Moreover, in flexible SRE-CG2 and in flexible MSDO-CG \hat{Z}_k is given respectively by

$$\hat{Z}_k = \hat{W}_k = \begin{cases} [T^t(\hat{r}_0)], & k = 1 \\ [T^{t/2}(\hat{r}_{k-1})], & k = \text{switchIt} \\ \hat{A} \hat{W}_{k-1}, & \text{else} \end{cases} \quad (4.4)$$

$$\hat{Z}_k = \hat{P}_k = \begin{cases} [T^t(\hat{r}_0)], & k = 1 \\ [T^t(\hat{r}_{k-1})] + \hat{P}_{k-1} \text{diag}(\beta_k), & 2 \leq k < \text{switchIt} \\ [T^{t/2}(\hat{r}_{k-1})], & k = \text{switchIt} \\ [T^{t/2}(\hat{r}_{k-1})] + \hat{P}_{k-1} \text{diag}(\beta_k), & \text{else} \end{cases} \quad (4.5)$$

and $\beta_k = -(\hat{A} \hat{P}_{k-1})^\top \hat{r}_{k-1}$. Noting that $\hat{r}_k = \hat{b} - \hat{A} \hat{x}_k = L^{-1}b - L^{-1}AL^{-\top}L^\top x_k = L^{-1}r_k$, then the corresponding equations for x_k , and r_k are:

$$\begin{aligned}\hat{\alpha}_k &= \hat{Z}_k^\top \hat{r}_{k-1} = \hat{Z}_k^\top L^{-1}r_k = (L^{-\top} \hat{Z}_k)^\top r_k \\ \hat{x}_k &= L^\top x_k = \hat{x}_{k-1} + \hat{Z}_k \hat{\alpha}_k = L^\top x_{k-1} + \hat{Z}_k \hat{\alpha}_k \implies x_k = x_{k-1} + (L^{-\top} \hat{Z}_k) \hat{\alpha}_k \\ \hat{r}_k &= L^{-1}r_k = \hat{r}_{k-1} - \hat{A} \hat{Z}_k \hat{\alpha}_k = L^{-1}r_{k-1} - L^{-1}AL^{-\top} \hat{Z}_k \hat{\alpha}_k \implies r_k = r_{k-1} - A(L^{-\top} \hat{Z}_k) \hat{\alpha}_k\end{aligned}$$

Let $Z_k = L^{-\top} \hat{Z}_k$, then

$$\begin{aligned}\hat{\alpha}_k &= Z_k^\top r_k, \\ x_k &= x_{k-1} + Z_k \hat{\alpha}_k, \\ r_k &= r_{k-1} - AZ_k \hat{\alpha}_k.\end{aligned}$$

As for the \hat{A} -orthonormalization, we require that $\hat{Z}_k^\top \hat{A} \hat{Z}_i = 0$ for some values of $i \neq k$. But

$$\hat{Z}_k^\top \hat{A} \hat{Z}_i = \hat{Z}_k^\top L^{-1}AL^{-\top} \hat{Z}_i = (L^{-\top} \hat{Z}_k)^\top A(L^{-\top} \hat{Z}_i) = Z_k^\top AZ_i.$$

Thus, it is sufficient to A-orthonormalize $Z_k = L^{-\top} \hat{Z}_k$ instead of \hat{A} -orthonormalizing \hat{Z}_k . Therefore, the recurrence formulae of $\hat{\alpha}_k, x_k$ and r_k in the preconditioned versions are identical to those of the unpreconditioned versions, and in both we A-orthonormalize a block of vectors Z_k . The only difference is in the construction of these block of vectors Z_k .

Since in (4.4) and (4.5), $T^j(\hat{r}_k) = T^j(L^{-1}r_k)$ and $\hat{A} \hat{Z}_{k-1} = L^{-1}AZ_{k-1}$ then respectively

$$Z_k = L^{-\top} \hat{Z}_k = L^{-\top} \hat{W}_k = W_k = \begin{cases} L^{-\top}[T^t(\hat{r}_0)], & k = 1 \\ L^{-\top}[T^{t/2}(\hat{r}_{k-1})], & k = \text{switchIt} \\ L^{-\top} \hat{A} \hat{W}_{k-1} = M^{-1}AW_{k-1}, & \text{else} \end{cases} \quad (4.6)$$

$$Z_k = L^{-\top} \hat{Z}_k = L^{-\top} \hat{P}_k = P_k = \begin{cases} L^{-\top}[T^t(\hat{r}_0)], & k = 1 \\ L^{-\top}[T^t(\hat{r}_{k-1})] + P_{k-1} \text{diag}(\beta_k), & 2 \leq k < \text{switchIt} \\ L^{-\top}[T^{t/2}(\hat{r}_{k-1})], & k = \text{switchIt} \\ L^{-\top}[T^{t/2}(\hat{r}_{k-1})] + P_{k-1} \text{diag}(\beta_k), & \text{else} \end{cases} \quad (4.7)$$

and $\beta_k = -(\hat{A} \hat{P}_{k-1})^\top \hat{r}_{k-1} = -(L^{-1}AP_{k-1})^\top L^{-1}r_{k-1} = (M^{-1}AP_{k-1})^\top r_{k-1} = (AP_{k-1})^\top M^{-1}r_{k-1}$.

Thus, preconditioned flexible SRE-CG2 algorithm is simply algorithm 3 where the definitions of W_k in lines 4,7,10 are modified based on (4.6). Preconditioned flexible MSDO-CG

is summarized in algorithm 5. Note that if the preconditioner is a block diagonal preconditioner, with t blocks that correspond to the initial t partitions of matrix A , then $[T^t(L^{-1}r_k)] = L^{-1}[T^t(r_k)]$ and $L^{-\top}[T^t(L^{-1}r_k)] = M^{-1}[T^t(r_k)]$. Similarly, $[T^{t/2}(L^{-1}r_k)] = L^{-1}[T^{t/2}(r_k)]$ and $L^{-\top}[T^{t/2}(L^{-1}r_k)] = M^{-1}[T^{t/2}(r_k)]$. In this case, no need for split preconditioning.

Algorithm 5 Split Preconditioned Flexible MSDO-CG

Input: A , $n \times n$ spd matrix; $M = LL^\top$, preconditioner; k_{max} , maximum iterations
 b , $n \times 1$ right-hand side; x_0 , initial guess; ϵ , stopping tolerance; switchTol
Output: x_k , approximate solution of the system $Ax = b$

- 1: $r_0 = b - Ax_0$, $\rho_0 = \|r_0\|_2$, $counter = 0$; $tol1 = 1$; $k = 1$;
- 2: **while** ($\rho_{k-1} > \epsilon \rho_0$ and $k < k_{max}$) **do**
- 3: **if** ($k == 1$) **then**
- 4: A-orthonormalize $P_1 = L^{-\top}[T^t(L^{-1}r_0)]$, let $V_1 = AP_1$ and $Q = P_1$
- 5: **else**
- 6: **if** ($tol1 < switchTol$ and $counter == 0$) **then**
- 7: $P_k = L^{-\top}[T^{t/2}(L^{-1}r_{k-1})]$;
- 8: $counter = 1$;
- 9: **else**
- 10: Let $\beta_k = -V_{k-1}^\top(M^{-1}r_{k-1})$ and $\hat{r}_{k-1} = L^{-1}r_{k-1}$
- 11: **if** ($counter == 0$) **then** Let $P_k = L^{-\top}[T^t(\hat{r}_{k-1})] + P_{k-1}diag(\beta_k)$
- 12: **else** Let $P_k = L^{-\top}[T^{t/2}(\hat{r}_{k-1})] + P_{k-1}diag(\beta_k)$
- 13: **end if**
- 14: **end if**
- 15: A-orthonormalize P_k against Q
- 16: A-orthonormalize P_k , let $V_k = AP_k$ and $Q = [Q P_k]$
- 17: **end if**
- 18: $\alpha_k = P_k^\top r_{k-1}$
- 19: $x_k = x_{k-1} + P_k \alpha_k$
- 20: $r_k = r_{k-1} - V_k \alpha_k$
- 21: $\rho_k = \|r_k\|_2$, $tol1 = (\rho_k - \rho_{k-1})/\rho_0$; $k = k + 1$
- 22: **end while**

5. Testing. The implementation of all the discussed methods depend on the A-orthonormalization procedures that are detailed in [17] and [7]. In all methods there is a need to A-orthonormalize some block of vectors against another block using CGS2 A-orthonormalization (Algorithm 18 in [17]) and then A-orthonormalize the block itself using Pre-CholQR [16] (Algorithm 23 in [17]).

We compare the convergence behavior of the different discussed truncated, restarted (section 5.1) and flexible enlarged CG (section 5.2) versions for solving the system $Ax = b$ using different number of partitions ($t = 2, 4, 8, 16, 32$, and 64 partitions). Moreover, we test the preconditioned versions (section 5.3). We first reorder/permute each matrix A using Metis's kway partitioning [13] for 128 subdomains. Then, the different larger subdomains for $t = 2, 4, 8, 16, 32, 64$ are defined by merging $128/t$ consecutive ones. The exact solution x is chosen randomly using online MATLAB's rand function (rand('twister', 5489); x = 4*rand(umeq,1);) and the right-hand side is defined as $b = Ax$. The initial iterate is set to $x_0 = 0$, and the stopping criteria tolerance is set to $tol = 10^{-8}$ for all the matrices.

We test the methods using the matrices NH2D, SKY2D, SKY3D, and ANI3D, that arise from different boundary value problems of convection diffusion equations, and generated

using FreeFem++ [10]. The main characteristics of the test matrices, including the condition number, number of CG iterations to convergence, and maximum allowed iterations k_{max} , are summarized in Table 5.1. For a detailed description of the test matrices, refer to [7].

Table 5.1: The test matrices

Matrix	Size	Nonzeros	2D/3D	Problem	Condition Number	CG Iterations	k_{max}
Nh2D	10000	49600	2D	Boundary value	6.01E+3	259	500
Sky3D	8000	53600	3D	Skyscraper	1.12E+6	902	1500
Ani3D	8000	53600	3D	Anisotropic Layers	2.01E+6	4179	5000
Sky2D	10000	49600	2D	Boundary value	2.91E+7	5980	6000

5.1. Truncated and Restarted Enlarged CG Methods. We start by comparing the convergence behavior of truncated and restarted SRE-CG2, MSDO-CG and Modified MSDO-CG for $trunc = 2, 20, 50$ and restart every $j = trunc$ iterations.

Table 5.2: Convergence (iteration **It**, relative error **RelErr**) of truncated and restarted SRE-CG2 versions, with respect to number of partitions **t**, truncation values **trunc**, and restart values **rstrt**.

	t	Truncated SRE-CG2						SRE-CG2		Restarted SRE-CG2			
		trunc = 2		trunc = 20		trunc = 50		trunc = k_{max}		rstrt = 20		rstrt = 50	
		It	RelErr	It	RelErr	It	RelErr	It	RelErr	It	RelErr	It	RelErr
Nh2D	2	241	2.6E-7	241	2.6E-7	241	2.6E-7	241	2.6E-7	-	6.1E-3	-	4.2E-5
	4	186	1.2E-7	186	1.2E-7	186	1.2E-7	186	1.2E-7	-	6.1E-3	-	6.1E-6
	8	147	5.3E-8	147	5.3E-8	147	5.3E-8	147	5.3E-8	-	5.0E-3	347	4.9E-7
	16	111	3.0E-8	111	3.0E-8	111	3.0E-8	111	3.0E-8	-	2.2E-3	247	2.7E-7
	32	82	2.3E-8	82	2.3E-8	82	2.3E-8	82	2.3E-8	-	7.9E-4	115	2.2E-7
	64	59	1.0E-8	59	1.0E-8	59	1.0E-8	59	1.0E-8	483	1.4E-6	62	2.4E-8
Sky3D	2	853	1.7E-5	839	1.7E-5	822	1.7E-5	569	1.3E-5	-	5.6E-1	-	2.5E-1
	4	759	1.2E-5	736	1.2E-5	707	1.2E-5	381	1.3E-5	-	5.2E-1	-	1.8E-1
	8	607	2.8E-6	566	2.7E-6	512	3.3E-6	212	1.5E-5	-	2.6E-1	-	1.1E-2
	16	424	1.4E-6	385	1.1E-6	310	1.6E-6	117	1.1E-5	-	1.6E-1	-	1.1E-3
	32	272	9.5E-7	214	1.0E-6	145	1.0E-6	68	1.2E-5	-	2.9E-2	501	1.4E-5
	64	154	5.5E-7	100	7.4E-7	42	8.7E-6	42	8.7E-6	1041	3.0E-5	42	8.7E-6
Ani3D	2	3961	4.1E-5	3968	3.9E-5	3899	4.6E-5	875	7.2E-5	-	5.2E-1	-	3.2E-1
	4	3523	4.5E-5	3526	3.9E-5	3516	3.9E-5	673	8.3E-5	-	5.2E-1	-	3.2E-1
	8	3127	4.6E-5	2771	5.3E-5	2677	5.9E-5	447	1.5E-4	-	3.8E-1	-	2.4E-1
	16	2413	3.0E-5	2006	3.1E-5	1738	3.1E-5	253	1.8E-4	-	3.8E-1	-	1.9E-1
	32	1636	1.8E-5	1214	1.7E-5	547	6.3E-5	146	2.8E-4	-	3.6E-1	1995	2.4E-4
	64	896	6.4E-6	457	1.5E-5	247	6.6E-5	91	1.7E-4	-	8.6E-2	922	1.1E-4
Sky2D	2	5476	3.7E-4	5420	3.7E-4	5357	3.6E-4	1415	7.4E-4	-	7.6E-1	-	6.8E-1
	4	4532	2.6E-5	4420	2.7E-5	4195	4.0E-5	754	2.2E-4	-	7.4E-1	-	6.5E-1
	8	2879	1.4E-5	2750	1.4E-5	2530	2.3E-5	399	1.7E-4	-	7.4E-1	-	6.1E-1
	16	1852	9.2E-6	1734	7.5E-6	1563	7.9E-6	225	1.0E-4	-	7.2E-1	-	5.3E-1
	32	984	5.0E-6	848	4.9E-6	662	5.4E-6	124	7.1E-5	-	6.4E-1	-	3.4E-1
	64	483	2.4E-6	364	2.6E-6	158	1.1E-5	73	4.4E-5	-	4.9E-1	2049	4.0E-3

The results are shown in Tables 5.2 and 5.3 for SRE-CG2 and MSDO-CG respectively. We do not show the results of the Modified MSDO-CG method as they are almost identical to that of MSDO-CG, with a difference of at most 10 iterations in a few cases.

The results of Truncated SRE-CG2 (Table 5.2) validate the theoretical discussion about W_k only needing to be A-orthonormalized to the previous 2 blocks. For the “well”-conditioned matrix NH2D, all the truncated versions converge in the same number of iterations. For the other 3 “ill”-conditioned matrices (in increasing order), we observe the effect of numerical loss of A-orthogonality of the truncated versions, where for larger $trunc$ values less iterations are required till convergence for the same t partitions. Moreover, in all cases and even for $trunc = 2$, Truncated SRE-CG2 converges in less iterations than CG. However, this is not the case for restarted SRE-CG2, where for restarting every $j = 20$ iterations the method doesn’t converge in k_{max} iterations to the relative residual tolerance of $tol = 10^{-8}$ ($\|r_k\|_2/\|r_0\|_2 < tol$). In the 2 cases where restarted SRE-CG2(20) converges, it requires more iterations than CG and a larger relative error than the truncated SRE-CG2 versions. Even restarted SRE-CG2(50) doesn’t converge in most cases for $t = 2, 4, 8, 16$ in k_{max} iterations or in less iterations than CG. This is due to the stagnation of the norm of residual when restarting.

For SRE-CG2, it is clear that Truncated SRE-CG2 for $trunc = 2$ converges in less iterations than the restarted version, and requires much less memory. However, the choice of the $trunc$ value affects the convergence behavior as shown in Figure 5.1 for the matrices SKY3D, SKY2D, and ANI3D with $trunc$ values from 2, 20, 50, 100, 200, 300, 400, k_{max} . Moreover, if it is possible to double the memory, then it is more efficient in terms of convergence to double t than $trunc$. Doubling the $trunc$ value doesn’t always lead to a proportional reduction in

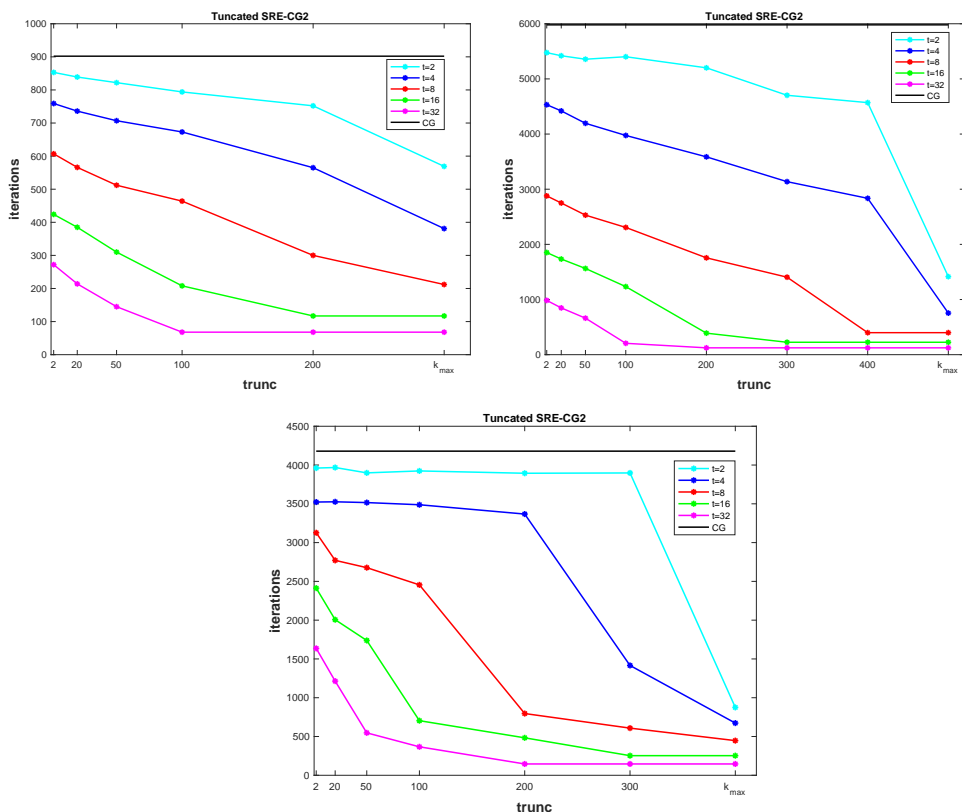


Fig. 5.1: Convergence of SRE-CG2($trunc$) for different $trunc$ and t values for matrices SKY3D (left), SKY2D (right), and ANI3D (bottom)

iterations. For example, the flat blue curve ($t = 4$) of matrix ANI3D shows that doubling $trunc$ from 50 to 100 to 200 barely reduces the iterations from 3516 to 3488 to 3368. We see a steep descent in number of iterations between $trunc = 200$ and 300. This steep descent occurs earlier for larger t , between $trunc = 100$ and 200 for $t = 8$, between $trunc = 50$ and 100 for $t = 16$, and between $trunc = 20$ and 50 for $t = 32$. For $t = 32$, SRE-CG(50) converges in 547 iterations, SRE-CG(100) converges in 704 iterations for $t = 16$, and SRE-CG(200) converges in 796 iterations for $t = 8$, all requiring the storage of 1600 vectors.

The case of MSDO-CG is different than SRE-CG2 since, as mentioned earlier, there is no guarantee that the method will converge with a truncated A-orthonormalization process. This is clear from the results in Table 5.3. For the NH2D matrix, all the truncated versions converge, but most requiring more iterations than CG, with less iterations for larger $trunc$ values. However, for the other 3 matrices the truncated MSDO-CG doesn't converge for $trunc = 2$. It converges only for SKY2D and ANI3D matrices with $trunc = 20, t = 64$, and

Table 5.3: Comparison of the convergence (iteration to convergence **It**, relative error **RelErr**) of truncated and restarted MSDO-CG versions, with respect to number of partitions t , truncation values $trunc$, and restart values $rstrt$.

	t	Truncated MSDO-CG						MSDOCG		Restarted MSDO-CG			
		trunc = 2		trunc = 20		trunc = 50		trunc = k_{max}		rstrt = 20		rstrt = 50	
		It	RelErr	It	RelErr	It	RelErr	It	RelErr	It	RelErr	It	RelErr
NH2D	2	301	6.4E-7	312	6.0E-7	314	6.4E-7	256	1.8E-7	-	6.7E-3	-	2.2E-6
	4	338	9.8E-7	328	1.1E-6	298	4.0E-7	206	1.3E-7	-	6.4E-3	-	4.9E-6
	8	380	9.9E-7	324	4.3E-7	240	3.6E-7	169	9.0E-8	-	5.1E-3	-	1.1E-6
	16	395	9.8E-7	275	7.7E-7	186	1.6E-7	139	3.7E-8	-	3.3E-3	401	5.5E-7
	32	373	1.3E-6	210	1.1E-6	131	2.5E-7	107	2.0E-8	-	1.5E-3	297	2.0E-7
	64	367	1.2E-6	155	5.8E-7	82	1.5E-7	77	1.0E-8	-	1.2E-3	177	1.2E-6
SKY3D	2	-	6.5E-3	-	5.7E-2	-	2.9E-3	646	1.6E-5	-	5.2E-1	-	1.5E-1
	4	-	3.1E-2	-	8.0E-2	-	3.4E-3	426	2.2E-5	-	4.8E-1	-	1.8E-1
	8	-	8.9E-2	-	2.7E-2	-	7.2E-4	231	2.3E-5	-	2.1E-1	-	8.2E-2
	16	-	8.1E-2	-	1.8E-2	-	1.2E-4	133	1.4E-5	-	1.3E-1	-	2.6E-2
	32	-	7.6E-2	-	8.5E-4	755	3.8E-6	79	8.7E-6	-	9.1E-2	916	1.7E-5
	64	-	2.6E-2	1294	6.9E-6	50	8.5E-6	50	8.5E-6	-	4.1E-3	50	8.5E-6
ANI3D	2	-	5.4E-3	-	2.5E-4	-	2.9E-4	933	7.0E-5	-	5.2E-1	-	3.7E-1
	4	-	2.9E-3	-	2.6E-4	-	2.4E-4	734	9.4E-5	-	5.0E-1	-	3.7E-1
	8	-	1.2E-3	-	3.4E-4	-	2.4E-4	471	2.1E-4	-	3.5E-1	-	2.7E-1
	16	-	4.2E-2	-	5.6E-4	-	2.1E-4	328	7.6E-5	-	3.5E-1	-	2.3E-1
	32	-	4.0E-2	-	3.1E-4	4347	3.3E-5	202	8.6E-5	-	3.0E-1	-	1.1E-1
	64	-	6.3E-2	4716	3.1E-5	1838	3.9E-5	116	1.3E-4	-	1.8E-1	-	6.8E-3
SKY2D	2	-	3.2E-2	-	3.9E-2	-	1.0E-1	1514	8.1E-4	-	7.5E-1	-	6.7E-1
	4	-	4.2E-2	-	2.5E-1	-	3.2E-2	845	3.3E-4	-	7.1E-1	-	6.2E-1
	8	-	7.6E-2	-	3.3E-1	-	1.1E-2	513	2.3E-4	-	6.8E-1	-	5.8E-1
	16	-	2.1E-1	-	3.4E-1	-	5.9E-3	291	2.2E-4	-	6.7E-1	-	5.3E-1
	32	-	1.3E-1	-	2.6E-2	-	1.7E-3	162	1.1E-4	-	6.4E-1	-	3.9E-1
	64	-	3.1E-1	-	3.3E-3	2653	4.6E-5	120	2.4E-5	-	5.3E-1	-	5.0E-2

$trunc = 50, t = 32, 64$, and for SKY3D matrix with $trunc = 50, t = 64$. Note that when restarting every $j = 20$ iterations, the method doesn't converge in k_{max} iterations for all the matrices. As for restarting every $j = 50$ iterations, the method converges in less iterations than CG for NH2D and SKY3D matrices and $t = 64$.

It is clear that truncating the A-orthonormalization process is better than restarting in the cases where the methods converge, as the truncated versions converge in less iterations. Moreover, the effect of the condition number of the matrices on the convergence of the different methods is clear, as the larger the condition number is, more iterations are required for convergence.

We also tested the restarted versions where the restart is done once the relative difference of residual norm is less than some $restartTol$ for $restartTol = 10^{-3}, 10^{-5}, 10^{-7}$. The results are shown in tables 5.4 and 5.5, where in addition to the number of iterations (**It**) to convergence and the corresponding relative error (**RelEr**), the number of restarts (**#r**) and the largest number of previous block vectors (**mem**) that are stored throughout the different restarted cycles are shown.

Table 5.4: Convergence (iteration to convergence **It**, relative error **RelEr**) of restarted SRE-CG2 versions, with respect to number of partitions **t**, restart tolerances **restartTol**. Moreover, the number of performed restarts **#r** and the largest restart cycle memory requirement **mem** are shown.

		SRE-CG2				Restarted SRE-CG2											
						restartTol = 10^{-3}				restartTol = 10^{-5}				restartTol = 10^{-7}			
						It	#r	mem	RelEr	It	#r	mem	RelEr	It	#r	mem	RelEr
t	It	mem	RelEr	It	#r	mem	RelEr	It	#r	mem	RelEr	It	#r	mem	RelEr		
NH2D	2	241	482	2.6E-7	387	10	174	9.1E-7	328	3	312	7.0E-7	247	1	286	3.3E-7	
	4	186	744	1.2E-7	470	14	244	1.6E-6	262	2	580	2.0E-7	195	1	616	1.9E-7	
	8	147	1176	5.3E-8	217	6	664	1.3E-6	178	2	992	8.4E-8	182	1	1152	5.3E-8	
	16	111	1776	3.0E-8	187	4	1184	1.7E-7	141	1	1184	8.5E-8	113	1	1568	7.1E-8	
	32	82	2624	2.3E-8	116	5	1792	1.7E-6	110	2	2240	3.0E-8	84	1	2368	3.4E-8	
	64	59	3776	1.0E-8	88	4	2752	2.0E-7	69	1	2880	2.9E-7	60	1	3520	1.3E-8	
SKY3D	2	569	1138	1.3E-5	1337	10	566	2.6E-5	793	2	838	8.7E-6	640	1	1064	1.7E-5	
	4	381	1524	1.3E-5	1238	11	816	4.2E-5	538	2	1388	9.1E-6	584	1	1232	9.4E-6	
	8	212	1696	1.5E-5	502	7	1584	4.2E-6	335	2	1664	6.8E-6	356	1	1624	8.4E-6	
	16	117	1872	1.1E-5	275	3	1712	1.5E-5	199	1	1824	1.2E-5	202	1	1792	4.0E-6	
	32	68	2176	1.2E-5	183	4	1888	2.0E-5	119	1	2016	1.4E-5	114	1	2080	2.5E-6	
	64	42	2688	8.7E-6	80	2	2240	1.5E-5	69	1	2240	1.1E-5	67	1	2560	1.8E-6	
Ani3D	2	875	1750	7.2E-5	4412	19	976	1.0E-4	1677	3	1290	1.1E-4	1238	1	1646	7.3E-5	
	4	673	2692	8.3E-5	2080	11	1340	1.9E-4	1011	2	1824	1.2E-4	876	1	2124	7.7E-5	
	8	447	3576	1.5E-4	1549	12	1808	1.3E-4	924	3	2480	1.2E-4	579	1	3480	1.4E-4	
	16	253	4048	1.8E-4	1181	15	2528	1.4E-4	517	2	3712	1.3E-4	362	1	3904	2.5E-4	
	32	146	4672	2.8E-4	559	8	4000	1.1E-4	261	2	4416	1.5E-4	252	1	4064	2.4E-4	
	64	91	5824	1.7E-4	256	6	4736	3.0E-4	124	1	5696	2.4E-4	143	1	5440	2.1E-4	
SKY2D	2	1415	2830	7.4E-4	6000	51	1460	4.9E-2	2903	3	2814	1.1E-4	1476	1	2830	1.1E-3	
	4	754	3016	2.2E-4	6000	41	2824	1.5E-3	1309	2	2984	3.7E-4	904	1	3024	3.4E-4	
	8	399	3192	1.7E-4	1653	13	3096	8.9E-5	799	2	3176	1.2E-4	498	1	3224	1.7E-4	
	16	225	3600	1.0E-4	1466	10	3264	1.6E-4	489	2	3472	1.3E-4	404	1	3440	1.1E-4	
	32	124	3968	7.1E-5	429	6	4000	6.9E-5	268	2	3872	3.3E-5	210	1	3584	4.9E-4	
	64	73	4672	4.4E-5	211	4	4672	3.0E-5	125	1	4800	2.6E-5	118	1	4224	1.8E-4	

As shown in Tables 5.4 and 5.5, using $restartTol = 10^{-3}$ leads to early and several restarts that might lead to stagnation in a few cases. Moreover, the total number of iterations is increased with respect to the non-restarted method, and in some cases for $t = 2, 4$ they require more iterations than CG. However, the memory reduction with respect to SRE-CG2 and MSDO-CG is between 20% and 60%. On the other hand, using $restartTol = 10^{-7}$ leads to a very late and mostly one restart, thus defeating the purpose of restart (reducing memory requirements). This is clear as the memory requirements for $t = 16, 32, 64$ of the restarted versions is almost identical to the initial versions. The moderate choice is setting $restartTol = 10^{-5}$ which leads to a few restarts without stagnation with a memory reduction of 5% to 50%. For some cases, even though for $restartTol = 10^{-5}$ the methods restart earlier and more than the case of $restartTol = 10^{-7}$, yet the needed memory is more. For example, SKY2D with $t = 16, 32, 64$, SKY3D with $t = 4, 8, 16$, and ANI3D with $t = 32$.

Comparing the restarted versions with a fixed restarted cycle (Tables 5.2 and 5.3) to the versions with the restart tolerance (Tables 5.4 and 5.5) it is clear that restarting once the relative difference of the residuals is less than some tolerance is more adaptive than fixing the

Table 5.5: Comparison of the convergence (iteration to convergence **It**, relative error **RelEr**) of restarted MSDO-CG versions, with respect to number of partitions **t**, restart tolerances **restartTol**. The number of performed restarts **#r** and largest restart cycle memory requirement **mem** are shown.

	t	MSDOCG				Restarted MSDO-CG											
		It	mem	RelErr	restartTol = 10^{-3}				restartTol = 10^{-5}				restartTol = 10^{-7}				
					It	#r	mem	RelEr	It	#r	mem	RelEr	It	#r	mem	RelEr	
Nh2D	2	256	512	1.8E-7	458	14	162	1.7E-6	301	3	278	1.3E-6	304	2	284	6.5E-7	
	4	206	824	1.3E-7	352	10	372	2.7E-6	266	2	592	5.9E-7	251	1	648	8.8E-7	
	8	169	1352	9.0E-8	302	6	720	6.6E-7	220	2	1048	3.8E-7	200	1	1152	5.4E-7	
	16	139	2224	3.7E-8	252	8	1232	1.2E-6	180	2	1696	2.7E-7	173	1	1952	5.2E-7	
	32	107	3424	2.0E-8	222	7	2048	5.0E-7	150	2	2784	1.3E-7	134	1	3136	3.7E-7	
	64	77	4928	1.0E-8	163	6	3328	1.9E-7	94	2	4096	7.0E-8	79	1	4672	1.4E-7	
Sky3D	2	646	1292	1.6E-5	-	11	668	9.3E-4	943	2	1000	2.4E-5	900	1	958	4.5E-5	
	4	426	1704	2.2E-5	-	14	1296	6.7E-5	730	2	1636	1.3E-5	739	1	1520	2.7E-5	
	8	231	1848	2.3E-5	953	9	1480	1.1E-5	346	2	1824	8.3E-6	398	1	1712	1.9E-5	
	16	133	2128	1.4E-5	339	4	2000	5.2E-6	239	2	2096	9.4E-6	227	1	2096	7.3E-6	
	32	79	2528	8.7E-6	153	2	2240	6.5E-6	140	1	2272	4.3E-6	131	1	2464	5.6E-6	
	64	50	3200	8.5E-6	95	2	2816	7.4E-6	85	1	2752	8.3E-6	82	1	3072	5.7E-6	
Ani3D	2	933	1866	7.0E-5	-	48	954	1.7E-4	1810	3	1278	7.7E-5	1571	2	1572	7.9E-5	
	4	734	2936	9.4E-5	4653	44	1080	1.5E-4	1493	4	1708	9.6E-5	944	1	2780	8.5E-5	
	8	471	3768	2.1E-4	3793	36	2560	8.7E-5	1092	3	3200	1.3E-4	709	1	3680	1.7E-4	
	16	328	5248	7.6E-5	1417	17	3648	6.3E-5	707	3	4656	7.0E-5	477	1	5008	1.2E-4	
	32	202	6464	8.6E-5	1059	13	4672	4.6E-5	281	1	6304	1.1E-4	302	1	6112	1.2E-4	
	64	116	7424	1.3E-4	399	5	6336	3.9E-5	227	2	6720	6.9E-5	202	1	7104	9.0E-5	
Sky2D	2	1514	3028	8.1E-4	-	59	2360	7.1E-4	2200	2	2962	9.1E-4	1839	1	3022	7.2E-4	
	4	845	3380	3.3E-4	4835	41	2796	5.0E-4	1374	2	3324	3.7E-4	973	1	3368	3.3E-4	
	8	513	4104	2.3E-4	1940	14	3472	3.0E-4	917	2	4016	1.7E-4	692	1	4088	2.6E-4	
	16	291	4656	2.2E-4	1201	14	4384	2.1E-4	569	2	4480	4.4E-4	539	1	4432	1.5E-4	
	32	162	5184	1.1E-4	443	7	4896	1.1E-4	327	2	5024	5.5E-5	289	1	4800	8.6E-4	
	64	120	7680	2.4E-5	316	5	7232	1.6E-5	185	1	7488	2.8E-5	217	1	7424	2.6E-5	

restart iteration, which leads to convergence within the k_{max} iterations. But this comes at the expense of requiring more memory storage than the fixed restart iteration.

To summarize, for SRE-CG2 theoretically it is possible to truncate the A-orthonormalization process for some preset $trunc$ value depending on the available memory. However, if this $trunc$ value is too small relative to the required iterations to convergence by SRE-CG2, then the truncated version will require much more iterations, but still less than CG as shown in Figure 5.1. Moreover, it is preferable to double t rather than $trunc$. For MSDO-CG, truncation doesn't necessarily lead to convergence, as it is not guaranteed theoretically. As for restarting after a fixed number of iterations, it leads to stagnation and the method may not converge in k_{max} iterations, even though it requires the same storage as the truncated versions. Restarting after the relative difference of the residuals is less than the restart tolerance, is more flexible as it leads to convergence within the k_{max} iterations and in less iterations than CG, but more iterations than the corresponding method. However, its memory requirement is not known beforehand.

5.2. Flexible Enlarged CG Methods. We test the convergence of flexible SRE-CG2 and MSDO-CG for different t values and $switchTol = 10^{-3}, 10^{-5}, 10^{-7}$ (Tables 5.6, 5.7).

Table 5.6: Convergence (iteration to convergence **It**, switch iteration **sIt**, relative error **RelEr**) of flexible SRE-CG2 with respect to number of partitions **t**, switch tolerances **switchTol**.

		SRE-CG2			Flexible SRE-CG2								
		t	It	RelErr	switchTol = 10^{-3}			switchTol = 10^{-5}			switchTol = 10^{-7}		
It	sIt				RelEr	It	sIt	RelEr	It	sIt	RelEr	It	sIt
Nh2D	2	241	2.6E-7	282	14	6.6E-7	293	42	1.3E-7	253	144	2.1E-7	
	4	186	1.2E-7	251	14	1.8E-7	207	107	1.2E-7	190	155	1.5E-7	
	8	147	5.3E-8	192	14	1.0E-7	177	35	1.0E-7	175	38	9.2E-8	
	16	111	3.0E-8	152	14	5.1E-8	114	75	4.6E-8	111	99	3.2E-8	
	32	82	2.3E-8	108	14	3.3E-8	96	32	2.8E-8	83	75	1.6E-8	
	64	59	1.0E-8	77	14	1.7E-8	60	46	1.6E-8	59	56	1.2E-8	
Sky3D	2	569	1.3E-5	710	19	3.0E-5	671	85	3.5E-5	679	108	2.1E-5	
	4	381	1.3E-5	577	18	1.3E-5	535	84	2.7E-5	399	309	2.3E-5	
	8	212	1.5E-5	368	15	1.2E-5	312	78	1.9E-5	253	153	1.4E-5	
	16	117	1.1E-5	200	13	2.1E-5	134	85	1.4E-5	117	113	1.2E-5	
	32	68	1.2E-5	107	14	1.7E-5	69	56	1.4E-5	68	66	1.3E-5	
	64	42	8.7E-6	60	12	7.4E-6	43	34	6.8E-6	42	41	9.0E-6	
Ani3D	2	875	7.2E-5	1233	19	7.4E-5	1206	53	7.1E-5	884	415	7.9E-5	
	4	673	8.3E-5	861	19	7.0E-5	754	142	6.9E-5	689	345	8.3E-5	
	8	447	1.5E-4	683	11	6.2E-5	597	115	6.5E-5	584	144	9.8E-5	
	16	253	1.8E-4	440	11	1.5E-4	392	63	2.0E-4	353	118	2.2E-4	
	32	146	2.8E-4	243	11	1.9E-4	216	39	1.9E-4	150	125	2.2E-4	
	64	91	1.7E-4	138	11	2.2E-4	116	35	2.4E-4	100	58	2.0E-4	
Sky2D	2	1415	7.4E-4	2396	15	7.4E-4	2416	22	6.7E-4	2415	61	5.9E-4	
	4	754	2.2E-4	1411	15	8.1E-4	1315	106	1.2E-3	1290	148	3.2E-4	
	8	399	1.7E-4	733	15	2.9E-4	710	44	4.6E-4	664	95	2.4E-4	
	16	225	1.0E-4	386	11	1.6E-4	326	79	1.6E-4	227	189	1.5E-4	
	32	124	7.1E-5	208	13	1.0E-4	169	55	1.2E-4	125	113	8.9E-5	
	64	73	4.4E-5	115	10	6.5E-5	84	50	5.0E-5	74	67	4.0E-5	

In Tables 5.6 and 5.7 we compare the convergence behavior (number of iterations to convergence **It** and the relative error **RelEr**) of Flexible SRE-CG2 with that of SRE-CG2. We also show the switch iteration, **switchIt**, at which the t value is halved.

Flexible SRE-CG2 and Flexible MSDO-CG have the same convergence behavior as SRE-CG2 and MSDO-CG, respectively, where for larger t the methods converge in less iterations with similar order of relative errors, that increase with the matrices' condition number. Flexible SRE-CG2 with a given t value is a mixture of SRE-CG2 with t and $t/2$ vectors per iteration (similarly for MSDO-CG). Thus, it is expected that the convergence of Flexible SRE-CG2 to be within the range of SRE-CG2 with t and $t/2$ vectors per iteration. To which end of the spectrum the Flexible SRE-CG2's convergence lies, depends on the values of t and $switchTol$ and the matrix's condition number.

Setting $switchTol$ to 10^{-3} leads to an early switch in the first 10 to 20 iterations, thus converging in number of iterations closer to SRE-CG2 with $t/2$ (sometimes slightly more). In this case, Flexible SRE-CG2 will require more iterations and less memory than SRE-CG2 with t as shown in Table 5.8, however, more memory than SRE-CG2 with $t/2$. Thus it is more efficient to use SRE-CG2 with $t/2$ rather than Flexible SRE-CG2 with t and $switchTol = 10^{-3}$.

Table 5.7: Convergence (iteration to convergence **It**, switch iteration **sIt**, relative error **RelEr**) of flexible MSDO-CG with respect to number of partitions t , restart tolerances **restartTol**.

		MSDOCG			Flexible MSDO-CG								
		t	It	RelErr	switchTol = 10^{-3}			switchTol = 10^{-5}			switchTol = 10^{-7}		
It	sIt				RelEr	It	sIt	RelEr	It	sIt	RelEr	It	sIt
N12D	2	256	1.8E-7	267	14	4.1E-7	257	58	4.5E-7	257	143	2.9E-7	
	4	206	1.3E-7	254	14	1.7E-7	229	58	2.0E-7	208	163	1.3E-7	
	8	169	9.0E-8	204	14	1.2E-7	183	69	1.3E-7	170	145	9.8E-8	
	16	139	3.7E-8	165	14	9.9E-8	152	56	9.9E-8	139	123	4.3E-8	
	32	107	2.0E-8	135	14	4.1E-8	117	57	1.9E-8	107	99	2.4E-8	
	64	77	1.0E-8	100	16	2.7E-8	93	27	2.7E-8	77	74	1.1E-8	
Sky3D	2	646	1.6E-5	751	18	2.2E-5	744	35	2.9E-5	660	479	3.1E-5	
	4	426	2.2E-5	650	23	1.4E-5	627	59	1.7E-5	441	380	2.3E-5	
	8	231	2.3E-5	412	17	1.9E-5	383	50	1.7E-5	238	214	1.7E-5	
	16	133	1.4E-5	219	16	1.5E-5	215	23	1.1E-5	133	131	1.5E-5	
	32	79	8.7E-6	120	14	1.9E-5	79	69	1.3E-5	79	77	9.2E-6	
	64	50	8.5E-6	68	11	1.5E-5	50	42	1.6E-5	50	48	9.3E-6	
Ant3D	2	933	7.0E-5	1232	19	8.0E-5	1172	107	6.9E-5	1036	271	6.6E-5	
	4	734	9.4E-5	917	19	6.8E-5	829	119	6.6E-5	750	249	7.4E-5	
	8	471	2.1E-4	733	20	8.5E-5	727	39	8.8E-5	605	249	1.7E-4	
	16	328	7.6E-5	452	21	2.1E-4	439	34	2.0E-4	342	164	1.8E-4	
	32	202	8.6E-5	320	10	6.8E-5	254	84	6.6E-5	231	111	9.9E-5	
	64	116	1.3E-4	186	17	1.1E-4	180	23	1.0E-4	123	91	2.0E-4	
Sky2D	2	1514	8.1E-4	2400	15	6.4E-4	2359	66	6.3E-4	2218	328	9.0E-4	
	4	845	3.3E-4	1497	15	5.4E-4	1469	46	8.3E-4	1392	131	7.8E-4	
	8	513	2.3E-4	830	15	2.8E-4	782	64	2.4E-4	671	181	4.3E-4	
	16	291	2.2E-4	503	11	2.1E-4	465	49	1.1E-4	291	262	2.2E-4	
	32	162	1.1E-4	277	13	2.9E-4	236	52	1.4E-4	163	150	1.4E-4	
	64	120	2.4E-5	150	13	9.9E-5	121	68	4.4E-5	120	101	2.5E-5	

On the other hand, setting $switchTol$ to 10^{-7} leads to a relatively late switch for $t = 16, 32, 64$, implying that the number of iterations is closer to that of SRE-CG2 with the same t . Moreover, in this case the memory reduction is minimal for matrices NH2D, SKY3D and SKY2D as shown in Table 5.8, but is between 5% and 20% for ANI3D.

As for $switchTol = 10^{-5}$, it is the moderate choice that balances between the number of iterations to convergence and the required memory, as the switch occurs earlier than the case of 10^{-7} and after that of 10^{-3} . Thus, number of iterations to convergence for $switchTol = 10^{-5}$ is less than that of $switchTol = 10^{-3}$ and greater than or equal to that of $switchTol = 10^{-7}$. The converse is observed for the memory requirements, since the switch iteration increases as $switchTol$ decreases. For $t = 16, 32, 64$, the reduction of memory of flexible SRE-CG2 with respect to SRE-CG2 with the same t is between 10% and 20% (between 10% and 20% for NH2D, 10% and 12% for SKY3D, 10% and 17% for ANI3D, and 10% for SKY2D). Note that for the matrices SKY2D and ANI3D with larger condition number requiring more iterations to convergence, leads to a larger number of vectors to be stored.

A similar convergence behavior is observed for MSDO-CG in Table 5.7, yet it requires more iterations than SRE-CG2, thus requiring more memory storage (Table 5.9)

Table 5.8: Memory requirements of SRE-CG2, restarted SRE-CG2, flexible SRE-CG2 and restarted flexible SRE-CG2 with respect to number of partitions t , and restart tolerances $restartTol$.

		SRE-CG2		Restarted, restartTol =						Flexible, switchTol =						Restarted flexible, restartTol =					
				10 ⁻³		10 ⁻⁵		10 ⁻⁷		10 ⁻³		10 ⁻⁵		10 ⁻⁷		10 ⁻³		10 ⁻⁵		10 ⁻⁷	
t	It	mem	It	mem	It	mem	It	mem	It	mem	It	mem	It	mem	It	mem	It	mem	It	mem	
			NH2D	2	241	482	240	452	282	480	247	288	282	296	293	335	253	397	264	250	287
4	186	744		198	736	260	612	195	620	251	530	207	628	190	690	242	456	286	428	196	620
8	147	1176		158	1152	175	1120	182	1152	192	824	177	848	175	852	198	736	219	736	215	708
16	111	1776		122	1728	141	1200	113	1584	152	1328	114	1512	111	1680	159	1160	156	1200	113	1584
32	82	2624		94	2560	108	2432	84	2400	108	1952	96	2048	83	2528	123	1744	134	1632	84	2400
64	59	3776		72	3712	69	2944	60	3584	77	2912	60	3392	59	3680	94	2560	70	2944	60	3584
Sky3D	2	569	1138	575	1112	623	1076	640	1064	710	729	671	756	679	787	718	699	755	670	763	655
	4	381	1524	391	1492	459	1500	584	1236	577	1190	535	1238	399	1416	570	1104	634	1100	632	1236
	8	212	1696	224	1672	287	1672	356	1624	368	1532	312	1560	253	1624	389	1496	451	1492	510	1428
	16	117	1872	130	1872	199	1824	202	1808	200	1704	134	1752	117	1840	224	1688	293	1664	207	1808
	32	68	2176	82	2176	119	2016	114	2112	107	1936	69	2000	68	2144	131	1872	167	1792	133	2112
	64	42	2688	54	2688	69	2240	67	2624	60	2304	43	2464	42	2656	80	2176	94	2176	81	2624
ANI3D	2	875	1750	893	1748	920	1734	1238	1646	1233	1252	1206	1259	884	1299	1266	1247	1302	1249	1615	1200
	4	673	2692	690	2684	804	2648	876	2124	861	1760	754	1792	689	2068	893	1748	1000	1716	1057	1424
	8	447	3576	457	3568	557	3536	579	3480	683	2776	597	2848	584	2912	684	2692	770	2620	776	2528
	16	253	4048	263	4032	313	4000	362	3904	440	3608	392	3640	353	3768	457	3568	506	3544	552	3472
	32	146	4672	157	4672	183	4608	252	4064	243	4064	216	4080	150	4400	263	4032	289	4000	355	4000
	64	91	5824	102	5824	124	5696	143	5440	138	4768	116	4832	100	5056	156	4640	178	4576	199	4512
Sky2D	2	1415	2830	1428	2826	1436	2828	1476	2830	2396	2411	2416	2438	2415	2476	2406	2391	2413	2391	2660	2599
	4	754	3016	769	3016	860	3016	904	3024	1411	2852	1315	2842	1290	2876	1431	2832	1521	2830	1563	2830
	8	399	3192	416	3208	444	3200	498	3224	733	2992	710	3016	664	3036	767	3008	795	3004	842	2988
	16	225	3600	232	3536	301	3552	404	3440	386	3176	326	3240	227	3328	409	3184	479	3200	587	3184
	32	124	3968	137	3968	180	4000	210	3616	208	3536	169	3584	125	3808	234	3536	276	3536	295	3616
	64	73	4672	83	4672	125	4800	118	4288	115	4000	84	4288	74	4512	133	3936	177	4064	160	4288

In Tables 5.8 and 5.9, we also show the convergence and memory requirements of two “restarted” versions, different than those of section 5.1. The first is restarted SRE-CG2 or MSDO-CG where once the relative residual norm is less than restartTol, the method is restarted with the same t value. The second is restarted flexible SRE-CG2 or flexible MSDO-CG where once the relative residual norm is less than restartTol, the method is restarted with the $t/2$ value. In both cases, the method is only restarted once and this restart occurs at the same switch iteration of flexible SRE-CG2 or flexible MSDO-CG.

Restarting SRE-CG2 with restartTol = 10^{-3} has a negligible effect on memory reduction, and in some cases ($t = 32, 64$ for SKY3D, ANI3D, SKY2D) no reduction at all, since after restarting, the method requires the exact number of iterations to converge as SRE-CG2. Decreasing restartTol increases the number of iterations to convergence, i.e. increases the runtime and performed flops, without significantly reducing the memory requirement. The same behavior is observed when comparing restarted Flexible SRE-CG2 to Flexible SRE-CG2. For restartTol = 10^{-7} or 10^{-5} , the restarted Flexible SRE-CG2 may converge in up to double the iterations of Flexible SRE-CG2 and reduce the memory requirement by at most 15%.

Table 5.9: Memory requirements of MSDO-CG, restarted MSDO-CG, flexible MSDO-CG and restarted flexible MSDO-CG with respect to number of partitions t , and restart tolerances restartTol.

		MSDOCG		Restarted, restartTol =						Flexible, switchTol =						Restarted flexible, restartTol =					
				10^{-3}		10^{-5}		10^{-7}		10^{-3}		10^{-5}		10^{-7}		10^{-3}		10^{-5}		10^{-7}	
	t	It	mem	It	mem	It	mem	It	mem	It	mem	It	mem	It	mem	It	mem	It	mem	It	mem
NI2D	2	256	512	256	484	277	438	293	300	267	281	257	315	257	400	263	249	270	212	313	286
	4	206	824	207	772	238	720	251	652	254	536	229	574	208	742	257	486	282	448	256	652
	8	169	1352	169	1240	213	1152	200	1160	204	872	183	1008	170	1260	209	780	245	704	205	1160
	16	139	2224	141	2032	172	1856	173	1968	165	1432	152	1664	139	2096	169	1240	202	1168	174	1968
	32	107	3424	109	3040	148	2912	134	3168	135	2384	117	2784	107	3296	140	2016	178	1936	135	3168
	64	77	4928	84	4352	93	4224	79	4736	100	3712	93	3840	77	4832	109	2976	118	2912	79	4736
Sky3D	2	646	1292	656	1276	675	1280	900	958	751	769	744	779	660	1139	717	699	732	697	900	958
	4	426	1704	448	1700	483	1696	739	1520	650	1346	627	1372	441	1642	655	1264	692	1266	818	1520
	8	231	1848	247	1840	280	1840	398	1712	412	1716	383	1732	238	1808	442	1700	474	1696	552	1712
	16	133	2128	148	2112	155	2112	227	2096	219	1880	215	1904	133	2112	247	1848	253	1840	276	2096
	32	79	2528	92	2496	140	2272	131	2464	120	2144	79	2368	79	2496	146	2112	188	2208	165	2464
	64	50	3200	60	3136	85	2752	82	3072	68	2528	50	2944	50	3136	89	2496	111	2688	106	3072
ANI3D	2	933	1866	949	1860	1025	1836	1178	1814	1232	1251	1172	1279	1036	1307	1266	1247	1349	1242	1497	1226
	4	734	2936	753	2936	847	2912	944	2780	917	1872	829	1896	750	1998	950	1862	1040	1842	1139	1780
	8	471	3768	490	3760	509	3760	709	3680	733	3012	727	3064	605	3416	750	2920	769	2920	904	2620
	16	328	5248	349	5248	361	5232	477	5008	452	3784	439	3784	342	4048	492	3768	504	3760	623	3672
	32	202	6464	211	6432	281	6304	302	6112	320	5280	254	5408	231	5472	338	5248	404	5120	427	5056
	64	116	7424	132	7360	138	7360	202	7104	186	6496	180	6496	123	6848	217	6400	222	6368	280	6048
Sky2D	2	1514	3028	1528	3026	1578	3024	1908	3160	2400	2415	2359	2425	2218	2546	2406	2391	2447	2381	2761	2433
	4	845	3380	859	3376	890	3376	1295	4656	1497	3024	1469	3030	1392	3046	1529	3028	1558	3024	1647	3032
	8	513	4104	527	4096	576	4096	939	6064	830	3380	782	3384	671	3408	858	3372	908	3376	1022	3364
	16	291	4656	302	4656	339	4640	539	4432	503	4112	465	4112	291	4424	524	4104	561	4096	753	4192
	32	162	5184	174	5152	211	5088	289	4800	277	4640	236	4608	163	5008	304	4656	341	4624	412	4800
	64	120	7680	132	7616	185	7488	217	7424	150	5216	121	6048	120	7072	174	5152	227	5088	255	6464

Comparing restarted SRE-CG2, Flexible SRE-CG2, and restarted Flexible SRE-CG2 for $\text{restartTol} = \text{switchTol} = 10^{-5}$, it is observed that restarted Flexible SRE-CG2 requires less memory than Flexible SRE-CG2, at the expense of more iterations to convergence. The rates of reduction in memory and increase in iterations differ with respect to the matrices and t values. Moreover, Flexible SRE-CG2 requires less memory than restarted SRE-CG2, and less iterations for $t = 16, 32, 64$. Thus, Flexible SRE-CG2 is the moderate choice that balances between the reduced memory and the augmented number of iterations. Moreover, in the case of MSDO-CG a similar convergence behavior is observed in Table 5.9, where it is clearer that the flexible version requires less memory and iterations than the restarted version.

5.3. Preconditioned versions. We test the preconditioned flexible SRE-CG2 and MSDO-CG with a Block Jacobi preconditioner.

Given the reordered/permutated matrix A using Metis's kway partitioning for 128 subdomains, we consider two options. The first is to define 64 subdomains by merging 2 consecutive ones. Then each of the 64 diagonal blocks of A is factorized using Cholesky decomposition (Table 5.10) or Incomplete Cholesky zero fill-in decomposition (Table 5.11).

The same preconditioner $M = LL^T$ is used for all the t values 2, 4, 8, 16, 32, 64, where L is given by (5.1) with the L_i 's being lower triangular blocks for $i = 1, 2, \dots, 64$,

$$L = \begin{bmatrix} L_1 & 0 & 0 & \dots & 0 \\ 0 & \ddots & 0 & \dots & 0 \\ 0 & 0 & L_i & \dots & 0 \\ 0 & 0 & 0 & \ddots & 0 \\ 0 & 0 & \dots & 0 & L_{64} \end{bmatrix}. \quad (5.1)$$

For each $t < 64$, the t blocks are the union of $64/t$ consecutive blocks.

The advantage of a block Jacobi preconditioner is that it is parallelizable without adding any layer of communication to the unpreconditioned algorithm, as processor/core i would compute its corresponding part of the output vector (or block of vectors) using the lower triangular block L_i . For example, computing $\hat{r}_k = L^{-1}r_k$ is equivalent to performing 64 independent forward substitutions, assuming L has the form (5.1). Computing $P_k = L^{-T}[T^t(\hat{r}_k)]$ is equivalent to performing 64 independent block backward substitutions. Similarly, computing $M^{-1}r_k$ is equivalent to performing 64 independent forward substitutions followed by 64 independent backward substitutions.

In Tables 5.10 and 5.11, the results for $\text{switchTol} = 10^{-5}$ and 10^{-7} are only shown, as similarly to the unpreconditioned case, setting switchTol to 10^{-3} leads to a very early switch (switch iteration = $O(10)$). Moreover, setting $\text{switchTol} = 10^{-7}$, leads to a late switch, and in some cases ($t = 64$) no switching occurs, implying no memory reduction. Thus again, $\text{switchTol} = 10^{-5}$ is the best option.

In general, by preconditioning, the number of iterations is significantly reduced, specifically for the ill conditioned matrices ANI3D (from 4179 to 73) and SKY2D (from 5980 to 283), implying a reduction in required memory in all the methods. Moreover, the obtained solution is better since the relative error is smaller $O(10^{-6})$, $O(10^{-7})$, $O(10^{-7})$, as compared to the unpreconditioned case $O(10^{-4})$, $O(10^{-5})$, $O(10^{-6})$ for the ill-conditioned matrices.

On the other hand, the difference between the Cholesky and Incomplete Cholesky Block Jacobi Preconditioner is that in the first, A_i , the diagonal block of the matrix A , is equal to $L_i L_i^T$ (up to numerical errors). However, in the Incomplete Cholesky version, the obtained lower triangular matrix L_i has the same sparsity pattern as the lower triangular part of A_i , but $A_i \neq L_i L_i^T$. Comparing the results of Incomplete Cholesky Block Jacobi Preconditioner in

Table 5.11 to that of Cholesky Block Jacobi Preconditioner in Table 5.10 shows an increase of 5% (ANI3D), 10% (SKY3D), 15% (SKY2D) and 20% (NH2D).

Note that for more parallelism when applying the preconditioner, it is possible to consider the 128 diagonal blocks and factorize each using Cholesky decomposition (Table 5.12) or Incomplete Cholesky zero fill-in decomposition (Table 5.13). Moreover, it is possible to reorder/permute the matrix A using Metis's kway partitioning with 256, 512, or 1024 partitions and use the corresponding diagonal blocks to define the preconditioner. However, with smaller diagonal blocks, and more off-diagonal information neglected, the preconditioner might become less efficient as it is not as good an approximation of A^{-1} , i.e. $A^{-1} = L^{-T}L^{-1} + Err$.

This effect can be seen Figures 5.2, 5.3, 5.4, and 5.5 where we plot the convergence (number of iterations) of preconditioned flexible SRE-CG2 (left) and flexible MSDO-CG (right) for $switchTol = 10^{-5}$ with different Block Jacobi preconditioners for $t = 4, 8, 16, 32, 64$. We compare the effect of using incomplete Cholesky (iChol) decomposition of the diagonal blocks A_i instead of the full Cholesky (Chol) decomposition, and compare the effect of using 64 diagonal blocks (Chol64, iChol64) versus 128 diagonal blocks (Chol128, iChol128).

Table 5.10: Convergence and memory requirements of Block Jacobi Cholesky 64 Preconditioned CG, SRE-CG2, flexible SRE-CG2, MSDO-CG, and flexible MSDO-CG and with respect to number of partitions $t = 2, 4, 8, 16, 32, 64$, and switch tolerances $switchTol = 10^{-5}, 10^{-7}$.

	CG	SRE-CG2				Flexible SRE-CG2, switchTol =								MSDOCG			Flexible MSDOCG, switchTol =							
						10^{-5}				10^{-7}							10^{-5}				10^{-7}			
		It	RE	It	mem	RelEr	It	sIt	mem	RelEr	It	sIt	mem	RelEr	It	mem	RelEr	It	sIt	mem	RelEr	It	sIt	mem
NH2D	91	3.81E-7	79	158	1.1E-7	93	16	109	1.4E-7	79	66	145	1.2E-7	79	158	2.7E-7	89	18	107	2.3E-7	79	68	147	3.2E-7
			64	256	8.5E-8	68	35	206	7.8E-8	64	57	242	8.2E-8	68	272	8.1E-8	72	43	230	7.8E-8	68	60	256	8.4E-8
			51	408	3.0E-8	51	35	344	6.2E-8	51	47	392	3.5E-8	56	448	5.9E-8	57	40	388	7.7E-8	56	51	428	7.3E-8
			39	624	2.3E-8	39	29	544	3.0E-8	39	37	608	2.3E-8	46	736	3.2E-8	46	35	648	4.9E-8	46	43	712	4.5E-8
			31	992	8.1E-9	31	24	880	1.5E-8	31	30	976	8.5E-9	35	1120	2.1E-8	38	17	880	2.7E-8	35	34	1104	2.2E-8
			24	1536	2.7E-9	24	20	1408	4.8E-9	24	-	1536	2.8E-9	27	1728	1.8E-8	28	24	1664	6.0E-9	27	-	1728	2.0E-8
Sky3D	227	1.41E-5	186	372	5.5E-6	202	42	244	1.3E-5	190	125	315	7.6E-6	210	420	1.4E-5	214	32	246	1.4E-5	214	147	361	1.5E-5
			156	624	1.7E-6	167	64	462	4.8E-6	157	113	540	7.6E-6	205	820	7.6E-6	227	13	480	8.3E-6	206	130	672	1.3E-5
			101	808	5.6E-7	127	40	668	4.9E-6	103	92	780	1.1E-6	141	1128	2.2E-6	177	31	832	7.1E-6	141	115	1024	1.2E-5
			56	896	5.3E-7	66	40	848	3.2E-7	56	-	896	5.3E-7	96	1536	8.2E-6	130	19	1192	1.2E-5	105	68	1384	1.2E-5
			34	1088	1.6E-7	40	18	928	8.7E-7	34	-	1088	1.6E-7	72	2304	1.6E-6	88	23	1776	4.5E-6	73	67	2240	5.8E-7
			22	1408	3.3E-7	22	18	1280	4.8E-7	22	-	1408	3.3E-7	45	2880	5.8E-7	63	10	2336	1.4E-6	45	-	2880	5.8E-7
ANI3D	73	1.17E-6	71	142	1.6E-6	73	19	92	1.3E-6	73	55	128	2.2E-6	73	146	3.4E-7	74	31	105	5.5E-7	73	57	130	3.6E-7
			66	264	1.2E-6	72	17	178	6.1E-7	67	54	242	7.6E-7	68	272	8.0E-7	70	26	192	5.2E-7	68	55	246	8.1E-7
			61	488	6.6E-7	67	22	356	8.0E-7	61	50	444	7.0E-7	66	528	6.7E-7	67	26	372	7.7E-7	66	55	484	6.8E-7
			56	896	1.0E-6	58	32	720	9.6E-7	56	44	800	1.7E-6	61	976	1.9E-6	63	29	736	1.1E-6	61	48	872	2.0E-6
			44	1408	7.3E-6	49	23	1152	3.9E-6	46	39	1360	4.5E-6	54	1728	3.9E-6	56	25	1296	3.4E-6	54	47	1616	4.4E-6
			36	2304	5.7E-6	38	22	1920	9.3E-6	37	31	2176	7.4E-6	43	2752	5.0E-6	47	23	2240	4.1E-6	43	39	2624	5.5E-6
Sky2D	283	1.21E-4	183	366	2.6E-4	230	26	256	1.7E-4	229	28	257	1.8E-4	239	478	1.8E-6	242	26	268	1.5E-4	221	124	345	6.4E-4
			106	424	9.1E-7	160	22	364	1.4E-4	106	94	400	1.2E-6	168	672	1.3E-6	201	25	452	2.7E-4	221	34	510	1.3E-6
			68	544	8.9E-7	89	23	448	1.3E-6	68	65	532	9.2E-7	117	936	1.7E-6	138	29	668	1.6E-6	117	116	932	1.7E-6
			44	704	6.4E-7	53	19	576	1.0E-6	44	42	688	6.7E-7	80	1280	6.2E-7	101	21	976	9.1E-7	80	-	1280	6.2E-7
			32	1024	5.3E-7	35	18	848	1.3E-6	32	-	1024	5.7E-7	52	1664	9.3E-7	69	16	1360	1.0E-6	52	-	1664	9.3E-7
			20	1280	4.7E-7	21	16	1184	5.3E-7	20	-	1280	5.6E-7	37	2368	3.5E-7	45	13	1856	4.2E-7	37	-	2368	3.5E-7

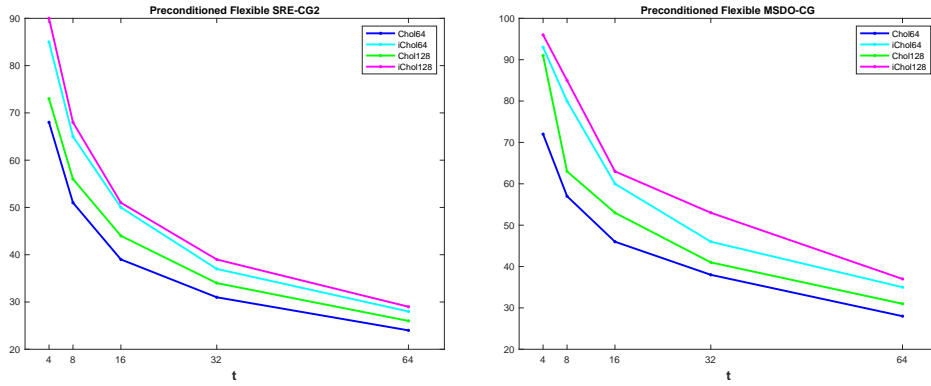


Fig. 5.2: Convergence of preconditioned flexible methods with switchTol = 10^{-5} for matrix NH2D

Table 5.11: Convergence and memory requirements of Block Jacobi Incomplete Cholesky 64 Preconditioned CG, SRE-CG2, flexible SRE-CG2, MSDO-CG, and flexible MSDO-CG and with respect to number of partitions $t = 2, 4, 8, 16, 32, 64$, and switch tolerances switchTol = $10^{-5}, 10^{-7}$.

	CG	SRE-CG2		Flexible SRE-CG2, switchTol =								MSDOCG			Flexible MSDOCG, switchTol =									
				10^{-5}				10^{-7}							10^{-5}				10^{-7}					
				It	mem	RelEr	It	sIt	mem	RelEr	It				sIt	mem	RelEr	It	mem	RelEr	It	sIt	mem	RelEr
Nh2D	116	3.19E-7	102	204	1.6E-7	118	34	152	2.2E-7	105	66	171	2.2E-7	109	218	2.3E-7	118	56	174	1.6E-7	111	75	186	1.6E-7
			81	324	1.1E-7	85	53	276	1.0E-7	81	71	304	1.5E-7	88	352	1.7E-7	93	56	298	9.3E-8	89	75	328	1.5E-7
			63	504	5.3E-8	65	44	436	6.0E-8	64	58	488	4.8E-8	72	576	4.7E-8	80	26	424	7.6E-8	72	65	548	5.6E-8
			49	784	2.0E-8	50	35	680	2.5E-8	49	45	752	2.4E-8	59	944	4.1E-8	60	45	840	3.7E-8	59	56	920	4.3E-8
			36	1152	1.8E-8	37	28	1040	1.9E-8	36	35	1136	1.8E-8	46	1472	2.2E-8	46	38	1344	3.0E-8	46	44	1440	2.6E-8
			28	1792	7.1E-9	28	23	1632	1.1E-8	28	-	1792	7.0E-9	35	2240	1.2E-8	35	31	2112	1.7E-8	35	-	2240	1.3E-8
Sky3D	250	1.04E-5	198	396	1.4E-5	225	26	251	1.6E-5	208	161	369	8.6E-6	250	500	1.2E-5	240	55	295	8.9E-6	258	195	453	1.0E-5
			164	656	3.1E-6	208	14	444	4.5E-6	168	131	598	2.9E-6	211	844	1.3E-5	229	34	526	2.1E-5	218	180	796	9.7E-6
			116	928	3.8E-7	141	41	728	3.4E-6	120	104	896	6.0E-7	146	1168	1.7E-5	199	22	884	4.7E-6	158	98	1024	9.3E-6
			65	1040	3.0E-7	90	32	976	2.1E-7	68	58	1008	4.3E-7	115	1840	3.7E-6	140	23	1304	8.3E-6	118	96	1712	3.3E-6
			39	1248	2.5E-7	41	32	1168	4.3E-7	39	-	1248	2.5E-7	80	2560	9.5E-6	90	28	1888	8.0E-6	81	76	2512	9.5E-6
			25	1600	2.6E-7	31	10	1312	2.8E-7	25	-	1600	2.7E-7	53	3392	3.6E-7	72	16	2816	2.6E-7	53	-	3392	3.6E-7
Ani3D	77	2.02E-6	75	150	6.5E-7	77	28	105	2.1E-6	78	61	139	8.2E-7	74	148	3.7E-7	79	27	106	5.2E-7	74	61	135	4.0E-7
			68	272	1.0E-6	69	28	194	5.8E-7	68	56	248	9.0E-7	70	280	8.0E-7	72	32	208	5.3E-7	70	58	256	8.0E-7
			64	512	7.3E-7	65	28	372	9.5E-7	64	52	464	6.8E-7	68	544	7.1E-7	68	31	396	7.4E-7	68	58	504	7.0E-7
			58	928	1.5E-6	62	26	704	7.8E-7	58	51	872	1.7E-6	63	1008	1.9E-6	63	31	752	1.4E-6	63	53	928	1.5E-6
			48	1536	4.6E-6	51	23	1184	4.4E-6	49	40	1424	4.6E-6	56	1792	3.8E-6	59	26	1360	2.8E-6	57	50	1712	2.9E-6
			38	2432	6.2E-6	40	24	2048	8.7E-6	39	33	2304	5.5E-6	47	3008	3.0E-6	49	23	2304	5.1E-6	48	42	2880	2.2E-6
Sky2D	325	1.61E-4	229	458	5.2E-6	267	28	295	4.6E-4	258	70	328	3.2E-4	299	598	1.2E-4	287	28	315	1.7E-4	262	112	374	8.2E-4
			139	556	6.7E-7	216	27	486	1.1E-6	147	100	494	1.2E-6	199	796	2.2E-6	260	18	556	7.7E-4	236	110	692	2.2E-6
			83	664	1.4E-6	113	26	556	1.4E-6	112	31	572	1.1E-6	140	1120	8.9E-7	180	19	796	1.3E-6	157	89	984	2.5E-6
			54	864	1.1E-6	62	23	680	1.7E-6	54	51	840	1.2E-6	98	1568	8.4E-7	132	20	1216	1.1E-6	117	41	1264	2.0E-6
			40	1280	2.7E-7	43	23	1056	7.0E-7	40	39	1264	3.0E-7	71	2272	1.9E-7	88	20	1728	5.5E-7	71	-	2272	1.9E-7
			25	1600	3.2E-7	25	20	1440	5.3E-7	25	-	1600	3.3E-7	46	2944	8.5E-7	62	17	2528	2.8E-7	46	-	2944	8.5E-7

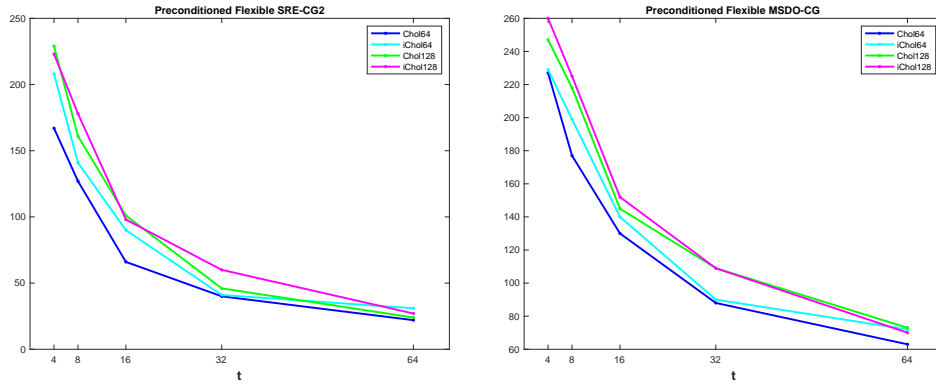


Fig. 5.3: Convergence of preconditioned flexible methods with switchTol = 10^{-5} for matrix SKY3D

Table 5.12: Convergence and memory requirements of Block Jacobi Cholesky 128 Preconditioned CG, SRE-CG2, flexible SRE-CG2, MSDO-CG, and flexible MSDO-CG and with respect to number of partitions $t = 2, 4, 8, 16, 32, 64$, and switch tolerances switchTol = $10^{-5}, 10^{-7}$.

	CG	SRE-CG2		Flexible SRE-CG2, switchTol =								MSDOCG			Flexible MSDOCG, switchTol =									
				10^{-5}				10^{-7}							10^{-5}				10^{-7}					
		It	RE	It	mem	RelEr	It	sIt	mem	RelEr	It	sIt	mem	RelEr	It	sIt	mem	RelEr	It	sIt	mem	RelEr		
Nh2D	101	2.77E-7	89	178	1.6E-7	96	37	133	2.2E-7	89	77	166	1.6E-7	92	184	1.5E-7	99	49	148	1.4E-7	92	78	170	1.5E-7
			71	284	7.6E-8	73	46	238	8.4E-8	71	62	266	8.0E-8	77	308	9.1E-8	91	8	198	1.4E-7	79	66	290	8.0E-8
			55	440	3.8E-8	56	39	380	4.7E-8	55	50	420	3.91E-8	62	496	7.0E-8	63	44	428	7.8E-8	62	56	472	8.0E-8
			43	688	2.4E-8	44	31	600	2.1E-8	43	40	664	2.5E-8	52	832	2.4E-8	53	39	736	3.6E-8	52	48	800	2.7E-8
			34	1088	1.3E-8	34	26	960	1.9E-8	34	33	1072	1.3E-8	40	1280	2.4E-8	41	32	1168	1.8E-8	40	39	1264	2.4E-8
			26	1664	7.5E-9	26	21	1504	1.3E-8	26	-	1664	7.6E-9	31	1984	1.1E-8	31	27	1856	1.8E-8	31	-	1984	1.3E-8
Sky3D	250	9.23E-6	210	420	1.4E-5	243	15	258	8.1E-6	221	103	324	1.3E-5	245	490	1.4E-5	252	60	312	1.4E-5	244	180	424	1.9E-5
			166	664	6.8E-6	229	15	488	3.4E-6	178	106	568	4.9E-6	230	920	8.7E-6	247	39	572	1.6E-5	251	94	690	1.0E-5
			119	952	2.8E-7	161	25	744	4.8E-6	119	101	880	8.4E-6	156	1248	3.3E-6	218	13	924	1.3E-5	161	128	1156	4.5E-6
			65	1040	2.5E-7	101	18	952	4.9E-7	65	65	1040	2.6E-7	116	1856	9.1E-6	145	22	1336	7.2E-6	130	68	1584	3.0E-6
			39	1248	2.3E-7	46	23	1104	5.2E-7	39	-	1248	2.3E-7	85	2720	5.8E-7	109	12	1936	7.6E-6	86	73	2544	3.6E-7
			24	1536	6.4E-7	24	21	1440	7.0E-7	24	-	1536	6.5E-7	53	3392	8.2E-7	73	15	2816	2.00E-6	56	48	3328	1.6E-7
Ani3D	77	5.8E-7	74	148	8.9E-7	76	31	107	7.3E-7	74	61	135	9.2E-7	75	150	4.4E-7	78	31	109	5.6E-7	76	61	137	4.0E-7
			68	272	6.19E-7	71	27	196	4.7E-7	69	51	240	6.7E-7	72	288	5.7E-7	73	32	210	4.9E-7	72	59	262	5.6E-7
			64	512	7.3E-7	70	22	368	6.7E-7	65	53	472	6.4E-7	71	568	4.3E-7	71	34	420	5.5E-7	71	59	520	4.6E-7
			58	928	1.8E-6	67	15	656	6.8E-7	59	47	848	1.7E-6	64	1024	2.3E-6	66	29	760	1.4E-6	65	54	952	1.2E-6
			48	1536	5.8E-6	51	30	1296	4.4E-6	50	40	1440	4.3E-6	58	1856	3.3E-6	60	27	1392	3.0E-6	58	49	1712	3.7E-6
			39	2496	6.3E-6	41	24	2080	1.1E-5	40	34	2368	5.7E-6	48	3072	3.5E-6	53	23	2432	2.5E-6	49	39	2816	2.9E-6
Sky2D	287	1.7E-4	201	402	6.6E-5	236	22	258	3.1E-4	230	34	264	2.9E-4	210	420	6.6E-4	246	30	276	2.1E-4	217	151	368	4.6E-4
			118	472	1.7E-6	174	27	402	1.6E-5	135	83	436	2.4E-6	176	704	1.5E-6	204	25	458	2.7E-4	221	71	584	1.9E-4
			74	592	1.5E-6	100	27	508	8.0E-7	74	72	584	1.6E-6	125	1000	1.8E-6	175	24	796	2.3E-6	125	124	996	1.8E-6
			49	784	1.0E-6	55	21	608	1.4E-6	49	47	768	1.0E-6	92	1472	3.7E-7	115	21	1088	1.1E-6	94	61	1240	1.6E-6
			37	1184	3.7E-7	40	20	960	8.2E-7	37	36	1168	3.4E-7	62	1984	2.1E-7	83	18	1616	2.2E-7	62	-	1984	2.1E-7
			23	1472	3.5E-7	23	17	1280	1.1E-6	23	22	1440	3.9E-7	42	2688	1.5E-7	56	15	2272	4.4E-7	42	-	2688	1.5E-7

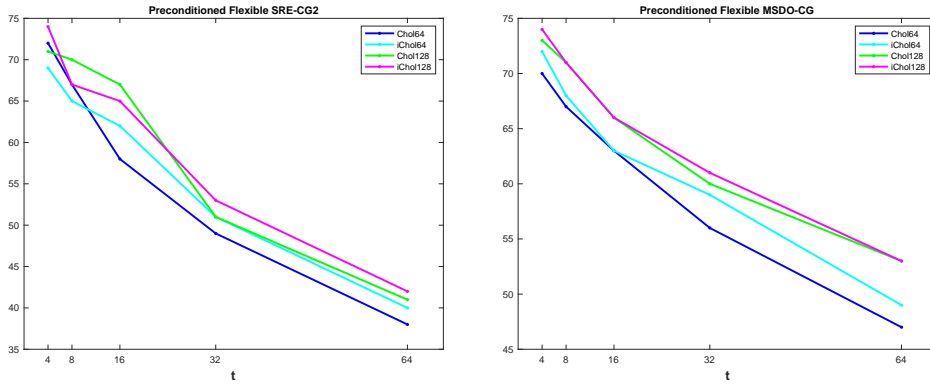


Fig. 5.4: Convergence of preconditioned flexible methods with switchTol = 10^{-5} for matrix ANI3D

Table 5.13: Convergence and memory requirements of Block Jacobi Incomplete Cholesky 128 Preconditioned CG, SRE-CG2, flexible SRE-CG2, MSDO-CG, and flexible MSDO-CG and with respect to number of partitions $t = 2, 4, 8, 16, 32, 64$, and switch tolerances switchTol = $10^{-5}, 10^{-7}$.

	CG	SRE-CG2			Flexible SRE-CG2, switchTol =								MSDOCG			Flexible MSDOCG, switchTol =								
		It	RE	RelEr	10^{-5}				10^{-7}				It	mem	RelEr	10^{-5}				10^{-7}				
					It	sIt	mem	RelEr	It	sIt	mem	RelEr				It	sIt	mem	RelEr	It	sIt	mem	RelEr	
Nh2D	119	4.95E-7	107	214	1.6E-7	115	59	174	2.4E-7	112	66	178	2.2E-7	114	228	1.8E-7	122	31	153	2.7E-7	114	93	207	1.9E-7
			86	344	8.8E-8	90	55	290	1.2E-7	87	72	318	8.0E-8	92	368	1.2E-7	96	59	310	1.4E-7	92	80	344	1.8E-7
			66	528	4.5E-8	68	46	456	5.0E-8	66	61	508	4.8E-8	74	592	8.0E-8	85	22	428	8.6E-8	75	68	572	5.6E-8
			51	816	2.4E-8	51	36	696	3.5E-8	51	47	784	2.5E-8	62	992	4.7E-8	63	47	880	3.9E-8	62	59	968	4.8E-8
			39	1248	9.1E-9	39	30	1104	1.4E-8	39	37	1216	9.4E-9	49	1568	2.3E-8	53	23	1216	3.4E-8	49	47	1536	2.4E-8
			29	1856	8.6E-9	29	24	1696	1.1E-8	29	28	1824	8.8E-9	37	2368	1.1E-8	37	32	2208	1.9E-8	37	-	2368	1.2E-8
Sky3D	266	1.00E-5	236	472	5.3E-6	251	20	271	1.0E-5	236	141	377	7.0E-6	265	530	1.9E-5	255	32	287	1.2E-5	271	144	415	1.7E-5
			180	720	3.8E-6	223	14	474	7.8E-6	177	141	636	9.8E-6	236	944	8.0E-6	260	22	564	1.1E-5	234	167	802	1.2E-5
			129	1032	5.6E-7	178	14	768	2.3E-6	136	104	960	4.1E-6	163	1304	2.3E-6	225	31	1024	7.0E-6	170	117	1148	1.1E-5
			72	1152	2.8E-7	98	34	1056	1.5E-6	73	68	1128	4.4E-7	126	2016	3.4E-6	152	20	1376	1.2E-5	128	105	1864	3.4E-6
			42	1344	5.1E-7	60	16	1216	4.6E-7	42	-	1344	5.1E-7	89	2848	8.0E-7	109	30	2224	1.4E-6	89	83	2752	8.2E-7
			27	1728	4.5E-7	27	25	1664	5.1E-7	27	-	1728	4.5E-7	57	3648	2.1E-7	70	28	3136	3.2E-6	60	51	3552	1.3E-7
Ani3D	77	1.08E-6	75	150	1.1E-6	77	32	109	1.2E-6	75	61	136	1.4E-6	76	152	3.8E-7	81	13	94	1.3E-6	76	62	138	3.7E-7
			68	272	7.0E-7	74	22	192	4.9E-7	69	54	246	7.1E-7	72	288	7.4E-7	74	32	212	5.4E-7	73	59	264	5.9E-7
			65	520	7.4E-7	67	27	376	8.5E-7	65	53	472	7.7E-7	71	568	5.2E-7	71	32	412	5.3E-7	71	58	516	5.2E-7
			59	944	1.5E-6	65	22	696	1.8E-6	60	51	888	1.8E-6	64	1024	2.1E-6	66	29	760	1.4E-6	64	54	944	1.8E-6
			49	1568	4.9E-6	53	28	1296	3.0E-6	50	40	1440	4.8E-6	59	1888	3.1E-6	61	28	1424	3.0E-6	60	50	1760	2.6E-6
			39	2496	7.8E-6	42	24	2112	8.3E-6	40	31	2272	8.8E-6	50	3200	2.0E-6	53	24	2464	3.4E-6	51	43	3008	1.5E-6
Sky2D	338	1.13E-4	240	480	7.5E-5	279	33	312	4.3E-4	264	134	398	2.0E-4	281	562	5.9E-4	276	33	309	6.6E-4	282	65	347	3.5E-4
			148	592	1.3E-6	226	30	512	2.0E-6	158	102	520	1.3E-6	195	780	2.7E-4	262	25	574	5.7E-4	301	36	674	9.9E-5
			87	696	1.4E-6	119	24	572	7.9E-7	87	83	680	1.4E-6	143	1144	1.4E-6	179	24	812	3.7E-4	153	99	1008	2.6E-6
			57	912	1.0E-6	67	23	720	2.5E-6	57	54	888	1.3E-6	101	1616	6.3E-7	132	23	1240	1.8E-6	101	100	1608	6.4E-7
			42	1344	3.4E-7	45	24	1104	9.0E-7	42	41	1328	3.7E-7	72	2304	7.1E-7	93	21	1824	1.1E-6	72	-	2304	7.2E-7
			26	1664	4.8E-7	27	20	1504	4.9E-7	26	25	1632	5.4E-7	50	3200	1.5E-7	63	17	2560	7.6E-7	50	-	3200	1.5E-7

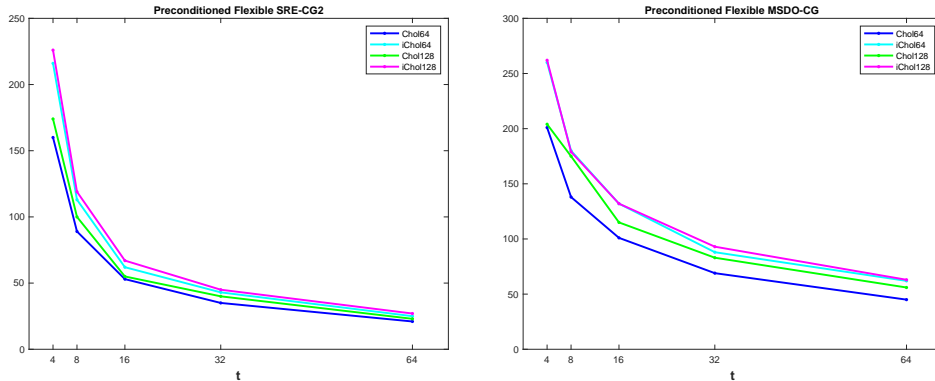


Fig. 5.5: Convergence of preconditioned flexible methods with $\text{switchTol} = 10^{-5}$ for matrix SKY2D

Clearly, the Cholesky Block Jacobi preconditioners reduces the iterations more than the incomplete Cholesky version (Chol64 vs iChol64, Chol128 vs iChol128). Similarly, using 64 blocks reduces the iterations more than 128 blocks (Chol64 vs Chol128, iChol64 vs iChol128).

Comparing the 4 versions (Chol64, iChol64, Chol128, iChol128) for the 4 matrices, Chol64 requires the least number of iterations whereas iChol128 requires the most number of iterations with an increase of around 30%. As for iChol64 and Chol128, for the matrices NH2D and SKY2D, Chol128 requires less iterations than iChol64, contrarily to the matrices AN13D and SKY3D.

6. Conclusion. In this paper we discussed different options for reducing the memory requirements of the introduced enlarged CG methods, specifically SRE-CG2 and MSDO-CG, without affecting much their convergence. We considered two options that require a fixed memory. The first is truncating the A-orthonormalization process, and the second is restarting after a fixed number of iteration. For SRE-CG2, it was proven theoretically [7] that it is possible to truncate the A-orthonormalization process for some preset *trunc* value. However, if this *trunc* value is too small relative to the required iterations to convergence by SRE-CG2, then the truncated version will require much more iterations, but still less than CG. For MSDO-CG, truncation doesn't necessarily lead to convergence, as it is not guaranteed theoretically. As for restarting after a fixed number of iterations, it leads to stagnation and the method may not converge in k_{max} iterations.

Thus, we introduced flexible enlarged versions where after some "switch" iteration, once the relative difference of residual norms is less than a given *switchTol*, the number of computed vectors is reduced to half. We proved that the flexible enlarged Krylov subspace is a superset to the classical Krylov subspace, thus the introduced methods will converge in less iterations than CG (which is validated in the numerical testings). Moreover, the convergence of the flexible methods is within the range of convergence of the corresponding methods with t and $t/2$ vectors per iteration. And it is observed that setting $\text{switchTol} = 10^{-5}$ is the moderate choice that balances between the reduced memory and the augmented iterations to convergence.

Accordingly, we tested some restarted versions based on the same switching condition. The first restarts every time the relative difference of the residuals is less than the restart tolerance. Unlike the restarted version with fixed restart iterations, it convergence within the k_{max} iterations and in less iterations than CG, but more iterations than the corresponding

method (up to double the iterations) where the memory is reduced. The second restarts only once. This reduces the augmented iterations of the first restarted version, but increases the memory requirements. The third is restarted flexible enlarged versions that restart only once, but t is halved after the restart. This further reduces the memory requirements, but at the expense of requiring more iterations than the second restarted version and the flexible version.

Hence, the introduced flexible enlarged methods with $\text{swichTol} = 10^{-5}$ are the moderate choice that balances between the reduced memory and the augmented iterations to convergence. Moreover, by preconditioning these flexible enlarged methods, the iterations to convergence are significantly reduced, further reducing the memory requirements.

REFERENCES

- [1] E. Carson. The adaptive s-step conjugate gradient method, SIAM J. Matrix Anal. Appl., 39(3):1318-1338, 2018.
- [2] A. Chapman and Y. Saad. Deflated and augmented Krylov subspace techniques. Numerical Linear Algebra Application (NLAA), 4(1):43-66, 1997.
- [3] A. T. Chronopoulos and W. Gear. s-step Iterative Methods For Symmetric Linear Systems. J. of Comput. Appl. Math., 25(2):153-168, 1989.
- [4] J. Demmel, M. Heath, and H. van der Vorst, Parallel Numerical Linear Algebra, Acta Numer., Cambridge University Press, Cambridge, UK, 111–197, 1993.
- [5] Jocelyne Erhel and Frédéric Guyomarc’h. An Augmented Conjugate Gradient Method for Solving Consecutive Symmetric Positive Definite Linear Systems. SIAM Journal on Matrix Analysis and Applications, 21(4):1279-1299, 2000
- [6] R. Fletcher. Conjugate gradient methods for indefinite systems. In G.A. Watson, editor, Numerical Analysis, volume 506 of Lecture Notes in Mathematics, pages 73–89. Springer Berlin Heidelberg, 1976.
- [7] L. Grigori, S. Moufawad, and F. Nataf. Enlarged Krylov Subspace Conjugate Gradient Methods for Reducing Communication. SIAM Journal on Matrix Analysis and Applications (SIMAX), 37(2):744-773, 2016
- [8] L. Grigori, O. Tissot. Reducing the communication and computational costs of Enlarged Krylov subspaces Conjugate Gradient. Research Report RR-9023, Inria Paris, 2017.
- [9] W. Gropp, Update on Libraries for Blue Waters, <http://jointlab.ncsa.illinois.edu/events/workshop3/pdf/presentations/Gropp-Update-on-Libraries.pdf>.
- [10] F. Hecht. New development in freefem++. Journal of Numerical Mathematics, 20(3-4):251-265, 2012.
- [11] M. R. Hestenes and E. Stiefel. Methods of conjugate gradients for solving linear systems. Journal of Research of the National Bureau of Standards, 49:409–436, 1952.
- [12] M. Hoemmen. Communication-Avoiding Krylov Subspace Methods. PhD thesis, EECS Department, University of California, Berkeley, 2010.
- [13] G. Karypis and V. Kumar, Metis 4.0: Unstructured graph partitioning and sparse matrix ordering system, Technical Report, Department of Computer Science, University of Minnesota, 1998.
- [14] P. Kogge, S. Borkar, D. Campbell, W. Carlson, W. Dally, M. Denneau, P. Franzone, W. Harrod, K. Hill, J. Hiller, S. Karp, S. Keckler, D. Klein, R. Lucas, M. Richards, A. Scarpelli, S. Scott, A. Snively, T. Sterling, R. S. Williams, and K. Yelick. ExaScale Computing Study: Technology Challenges in Achieving Exascale Systems. Technical Report. Available online at https://cpb-us-w2.wpmucdn.com/sites.gatech.edu/dist/5/462/files/2016/08/exascale_final_report_100208.pdf. September 2008.
- [15] C. Lanczos. Solution of systems of linear equations by minimized iterations. J. Res. Natl. Bur. Stand., 49:33-53, 1952.
- [16] B. Lowery and J. Langou. Stability Analysis of QR factorization in an Oblique Inner Product. ArXiv e-prints. <https://arxiv.org/abs/1401.5171>. January 2014.
- [17] S. Moufawad. Enlarged Krylov Subspace Methods and Preconditioners for Avoiding Communication. PhD thesis, Université Pierre et Marie Curie-Paris VI, 2014.
- [18] S. Moufawad. s-Step Enlarged Krylov Subspace Conjugate Gradient Methods. SIAM Journal on Scientific Computing, 42(1):A187-A219, 2020.
- [19] D. P. O’Leary. The block conjugate gradient algorithm and related methods. Linear Algebra and Its Applications, 29:293-322, 1980.
- [20] M. Rozložnik, M. Tuma, A. Smoktunowicz, and J. Kopal. Numerical stability of orthogonalization with a non-standard inner product. BIT Numerical Mathematics, 52(4):1035-1058, December 2012.
- [21] Y. Saad. Analysis of augmented Krylov subspace methods. SIAM Journal on Matrix Analysis and Applications, 18(2):435-449, 1997.

- [22] Y. Saad and M. H. Schultz. Gmres: a generalized minimal residual algorithm for solving nonsymmetric linear systems. SIAM J. Sci. Stat. Comput., 7(3):856–869, July 1986.
- [23] H. Van der Vorst. Bi-CGSTAB: A Fast and Smoothly Converging Variant of Bi-CG for the Solution of Nonsymmetric Linear Systems. SIAM Journal on Scientific and Statistical Computing, 13(2):631-644, 1992
- [24] J. Van Rosendale. Minimizing inner product data dependence in conjugate gradient iteration. In Proceeding IEEE International Conference on Parallel Processing, 1983.